Cotecmar

Vol. 4 - n.° 7 - July 2010

ISSN 1909-8642

Ship Science & Technology

SHIP SCIENCE & TECHNOLOGY

CIENCIA & TECNOLOGÍA DE BUQUES

ISSN 1909-8642

COTECMAR
COLOMBIA

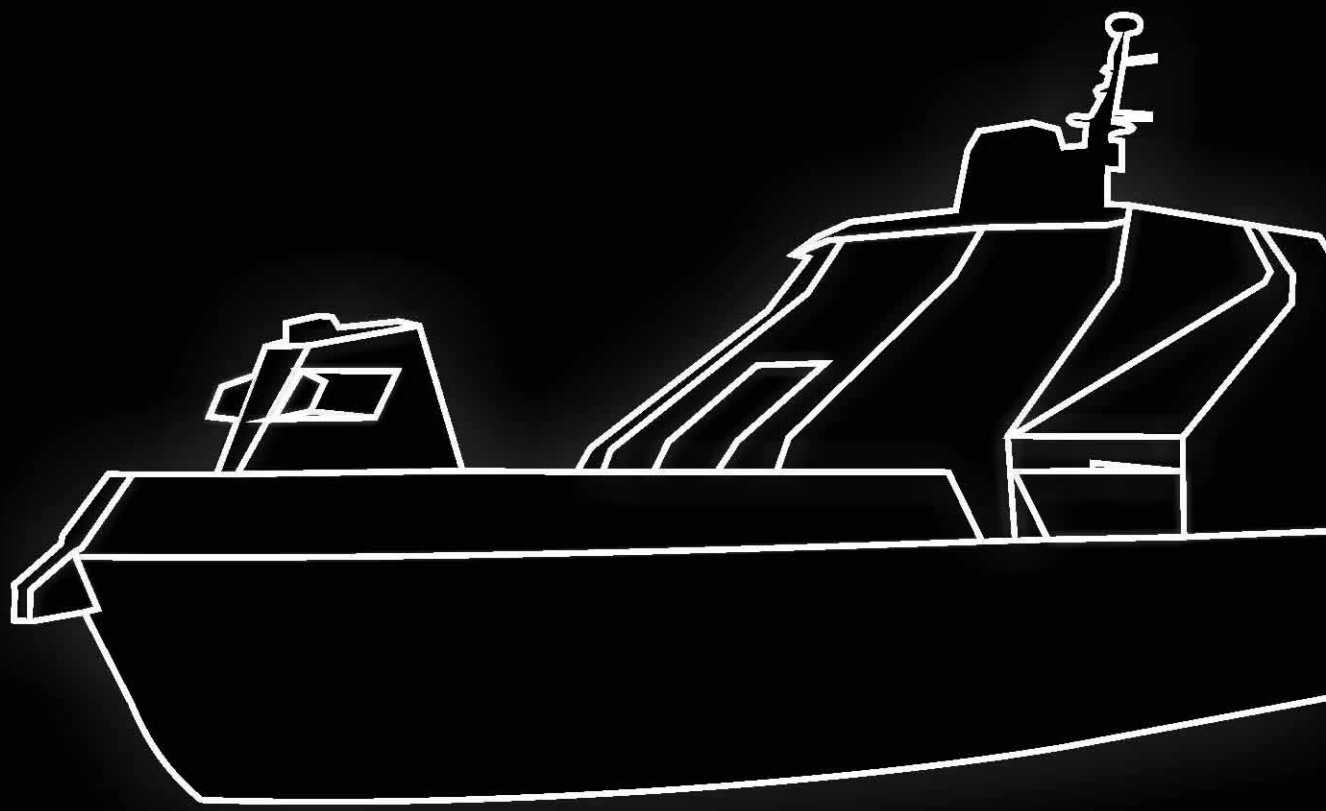

Vol. 4 - n.° 7
(1 - 70) July 2010

SHIP
SCIENCE & TECHNOLOGY
CIENCIA & TECNOLOGÍA DE BUQUES

Volume 4, Number 7 July 2010 ISSN 1909-8642

Ship Science & Technology is a specialized journal in topics related to naval architecture, and naval, marine and ocean engineering. Every six months, the journal publishes scientific papers that constitute an original contribution in the development of the mentioned areas, resulting from research projects of the Science and Technology Corporation for the Naval, Maritime and Riverine Industries, and other institutions and researchers. It is distributed nationally and internationally by exchange or subscription.

A publication of

Corporación de Ciencia y Tecnología para el Desarrollo de la Industria Naval, Marítima y Fluvial - Cotecmar
Electronic version: www.cotecmar.com/cytbuques/

Editorial Coordinator
Karen Domínguez Martínez. MMSc. (c)
Jimmy Saravia Arenas. MMSc. (c)

Layout and design
Mauricio Sarmiento Barreto

Printed by
Publicidad & Marketing. Bogotá, D.C.

SHIP
SCIENCE & TECHNOLOGY
CIENCIA & TECNOLOGÍA DE BUQUES

Volume 4, Number 7 July 2010 ISSN 1909-8642

Special Note
Nota Especial

Scientific and Technological Research Articles
Artículos de investigación científica y tecnológica

SHIP
SCIENCE & TECHNOLOGY
CIENCIA & TECNOLOGÍA DE BUQUES

Editorial Note

Cartagena de Indias, 21 July 2010.

Welcome to this special edition of the *Ship Science & Technology* journal. Through this special edition it is our privilege to bring together an excellent compilation of the strongest articles presented by the Panamerican Advanced Studies Institute (PASI). We are proud to announce that for the first time, this event was hosted in Colombia and hope that delegates found the event to be stimulating and a valuable of opportunity to network and keep abreast with developments in the field. This special edition is introduced by Dr. Leigh McCue from Virginia Tech and Dr. Marco San Juan from Universidad del Norte whose dedication, vision and hard work during the last two years made this event possible.

This PASI focused on the Dynamics and Control of Manned and Unmanned Marine Vehicles, a topic of special relevance to us, as it is in full alignment with Cotecmar's objective to increase awareness and develop the necessary knowledge to build a strong maritime industry in Colombia. Throughout the two weeks duration of this event, delegates had the opportunity to enhance their knowledge about the modern challenges and solutions faced by marine dynamics and control issues, establish collaborative relationships, and make new friends amongst colleagues. These new relationships have already resulted in new collaborative ventures amongst some of the institutions that took part in this year's PASI.

Having said this, I would like to take this opportunity to thank our partner, Universidad del Norte, for hosting the first week of the PASI in Barranquilla, and to thank Escuela Naval "Almirante Padilla", for hosting the second week in Cartagena. The hospitality of both these institutions made it possible for speakers and delegates alike to put to good practice the words from Cotecmar's Vicepresident, Captain Jorge E. Carreño, during the inaugural event: "while you learn about marine dynamics, take some time to enjoy these two unique cities in Colombia, enjoy the sun, the beaches, the food, the music, and in general take the time to experience the dynamics of the tropic".

Commander OSCAR DARÍO TASCÓN

SHIP
SCIENCE & TECHNOLOGY
CIENCIA & TECNOLOGÍA DE BUQUES

Nota Editorial

Cartagena de Indias, 21 de Julio de 2010.

Bienvenidos a esta edición especial de la revista *Ciencia y Tecnología de Buques*. En este número tenemos el privilegio de ofrecer una colección de algunos de los mejores artículos científicos presentados durante el primer Panamerican Advanced Studies Institute – PASI que ha tenido lugar en Colombia. La edición es introducida por la Dra. Leigh McCue de Virginia Tech y el Dr. Marco San Juan de la Universidad del Norte, los Investigadores Principales en este evento, cuya visión, trabajo y dedicación durante los últimos dos años hizo posible el mismo.

Este PASI en Dinámica y Control de Vehículos Tripulados y No Tripulados está completamente alineado con el objetivo de Cotecmar de incrementar el interés y el conocimiento requerido para construir una fuerte industria naval en Colombia. Durante dos semanas quienes asistieron al evento aprendieron más acerca de los retos modernos y las soluciones a los problemas en dinámica marina y control, construyeron nuevas relaciones colaborativas e hicieron nuevos amigos entre sus colegas. Estas nuevas relaciones han dado nacimiento a nuevos esfuerzos de colaboración entre las instituciones que estuvieron representadas en el evento.

Habiendo dicho esto, quisiera aprovechar la oportunidad para agradecer a nuestro socio, la Universidad del Norte, por haber recibido el evento durante la primera semana en Barranquilla, y agradecer a la Escuela Naval "Almirante Padilla", por haber hecho lo propio durante la segunda semana en Cartagena. Gracias a su hospitalidad, tanto instructores como los participantes pudieron tomarse en serio las palabras del Vicepresidente de Cotecmar, Capitán de Navío Jorge Enrique Carreño, durante la apertura del evento: "mientras aprenden sobre dinámica y control, tómense un tiempo para disfrutar estas dos ciudades únicas en Colombia, disfruten el sol, las playas, la comida, la música, y en general tómense el tiempo para experimentar la dinámica del trópico".

Capitán de Fragata OSCAR DARÍO TASCÓN

Concepts and Conclusions from the "2010 Pan-American Advanced Studies Institute on Dynamics and Control of Manned and Unmanned Marine Vehicles"

Conceptos y conclusiones de la "Sesión 2010 del Instituto Panamericano de Estudios Avanzados en Dinámica y Control de Vehículos Marinos tripulados y no tripulados"

Leigh McCue[1]
Marco Sanjuan[2]
Ryan Hubbard[3]

Abstract

In the summer of 2010, the first ever NSF's Pan-American Advanced Studies Institute (PASI) in Colombia was held in Barranquilla and Cartagena. The two-week institute brought together researchers of the Americas to discuss topics related to dynamics and control of manned and unmanned marine vehicles. This paper presents a summary of the program organization and findings, along with lecturer and participant feedback. It is intended to serve as a lead-in to the technical papers by PASI participants contained in this special edition of *Ship Science & Technology*.

Key words: PASI, marine vehicles, autonomous, unmanned.

Resumen

Entre los meses de Junio y Julio de 2010 se realizó por primera vez en Colombia el Instituto Panamericano de Estudios Avanzados (PASI, del inglés *Pan-American Advanced Studies Institute*) de la *National Science Foundation* (NSF), en las ciudades de Barranquilla y Cartagena. Este instituto a lo largo de dos semanas congregó a investigadores de todo el continente para discutir temáticas relacionadas con dinámica y control de vehículos marinos tripulados y no tripulados. Este artículo presenta una síntesis de los principales elementos de dicho instituto, los resultados de la organización del evento, así como la retroalimentación recibida por conferencistas y participantes. Además, este artículo pretende servir como prólogo a artículos técnicos preparados por los participantes del PASI en esta edición especial de Ciencia y Tecnología de Buques.

Palabras claves: PASI, vehículos marinos, autónomos, no tripulados.

Date received: July 16th, 2010. - *Fecha de recepción: 16 de Julio de 2010.*
Date Accepted: July 19th, 2010. - *Fecha de aceptación: 19 de Julio de 2010.*

[1] Aerospace and Ocean Engineering, Virginia Tech. e-mail: mccue@vt.edu
[2] Mechanical Engineering, Universidad del Norte. e-mail: msanjuan@uninorte.edu.co
[3] Aerospace and Ocean Engineering, Virginia Tech. e-mail: hubbard7@vt.edu

Introduction

The purpose of the Pan-American Advanced Studies Institute (PASI) on Dynamics and Control of Manned and Unmanned Marine Vehicles was to draw world leaders at controlling, modeling, and predicting the motions of marine vehicles in a unified setting to disseminate knowledge to students, researchers, academics, and practitioners in the Americas. The organization of the Institute represents collaboration between American academics at Virginia Tech and the University of Michigan, Colombian industry and academia including Cotecmar, Universidad del Norte, and Escuela Naval "Almirante Padilla," and Brazilian faculty at Universidade Federal do Rio de Janeiro.The Institute sought to broaden the base and expertise of researchers, scientists, and students studying dynamics and control as applied to marine vehicles as well to bring together researchers from different sectors of the marine field. By encouraging discussion, education, and collaboration through this Institute, the group collectively formed a stronger collective understanding of the dynamic behavior of vessels in marine environments, control system solutions, as well as the challenges ahead in analytical and computational modeling, design, and control of such vessels. Additionally, the PASI highlighted opportunities for use of unmanned vehicles in K-12 and undergraduate education particularly through SeaPerch (SNAME, 2010) and AUVSI (AUVSI, 2010) opportunities. In Fig. 1 the primary theme areas for the Institute; namely, manned vehicles, unmanned vehicles, and education and outreach, along with sub-topics are presented. Numerous topics appear at the intersection between manned and unmanned vehicles; one of the missions of this workshop was to encourage discussion between manned and unmanned vehicle researchers.

Program and organization

The PASI on dynamics and control of manned and unmanned marine vehicles was developed to educate graduate students and researchers on modern challenges and solutions to maritime dynamics and controls issues. Additionally, as part of the PASI, new collaborative relationships for researchers in the field of stability and control of marine vehicles throughout the Americas were built while bringing together scholars from traditionally disparate sectors of the maritime field, from exploration, to military and commercial shipping, to unmanned vehicles and robotics, in a single venue. Attendees came from as far north at Michigan, west as Hawaii, south as Brazil, and east as Spain. Substantial emphasis was also placed upon mechanisms for incorporation of

Fig. 1. Theme Areas for PASI on Dynamics and Control of Manned and Unmanned Marine Vehicles

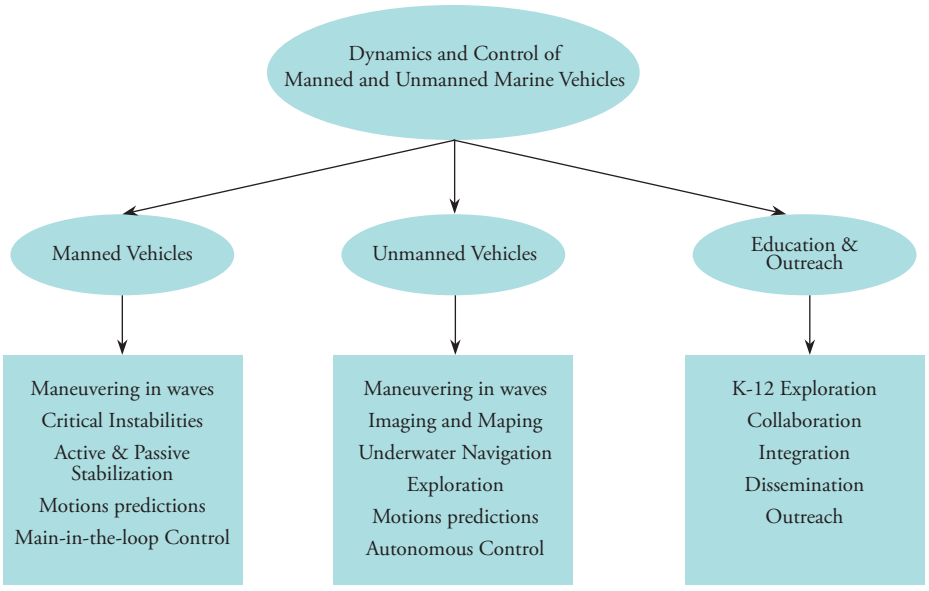

unmanned and autonomous vehicles into K-12 and undergraduate education such as the SeaPerch program and Association for Unmanned Vehicle Systems International (AUVSI) competitions.

Organizing Committees

The membership of the international and local organizing committees is as given in Table 1.

Table 1. International and local organizing committees

International Organizing Committee	Institution	Local Organizing Committee	Institution
Leigh McCue Marco Sanjuan Marcelo Santos Neves	Virginia Tech Universidad del Norte Universidade Federal do Rio de Janeiro	Marco Sanjuan Oscar Tascón Jorge Carreño	Universidad del Norte Cotecmar Cotecmar
Oscar Tascón	Cotecmar	Germán García	Escuela Naval "Almirante Padilla"
Armin Troesch	University of Michigan	Fabio Zapata	Escuela Naval "Almirante Padilla"

Program

A schedule of events from the final PASI program appears in Table 2. The program generally sought to focus upon manned vehicles in the first week and unmanned vehicles in the second week with lecturers highlighting overlap and areas for collaboration between researchers operating in either or both of these domains. Participants attended both weeks of the PASI to ensure cross-pollination of ideas.

Participants also engaged in the design and construction of a SeaPerch underwater vehicle. SeaPerch (SNAME, 2010) is a hands-on underwater robotics program coordinated by the Society of Naval Architects and Marine Engineers (SNAME) under Office of Naval Research (ONR)

Table 2. PASI 2010 Schedule

<table>
<tr><th></th><th>Sunday</th><th>Monday</th><th>Tuesday</th><th>Wednesday</th><th>Thursday</th><th>Friday</th><th>Saturday</th></tr>
<tr><td>Time</td><td>June 27</td><td>June 28</td><td>June 29</td><td>June 30</td><td>July 1</td><td>July 2</td><td>July 3</td></tr>
<tr><td>8:00am-9:45am</td><td></td><td rowspan="2">Registration, Logistics</td><td>McCue</td><td rowspan="2">Free</td><td>Santos Neves</td><td>Epureanu</td><td>Free</td></tr>
<tr><td>9:45am-10:00am</td><td rowspan="6">BAQ Airport to Hotel Transportation</td><td>Break</td><td>Break</td><td>Break</td><td></td></tr>
<tr><td>10:00am-12:00pm</td><td>Opening ceremony</td><td>Nonlinear Dynamics Presentations: Villagomez Rosales, Manuico Vivanco, Piro & Dorger, Sefat; Mod: Caldwell</td><td rowspan="5">River Trip</td><td>AUV Control Presentations: Caldwell, Andonian, McCarter, Rader*; Mod: Bula</td><td>CFD & Naval Architecture Presentations: Bula, Martin, Celis Carbajal, Backlund; Mod: Jones</td><td rowspan="5">Barranquilla to Cartagena (2 Stops)</td></tr>
<tr><td>12:00pm-2:00pm</td><td colspan="2">Lunch</td><td colspan="2">Lunch</td></tr>
<tr><td>2:00pm-3:45pm</td><td>Hansen</td><td>Troesch</td><td>Sanjuan</td><td>Wrap Up 1</td></tr>
<tr><td>3:45pm-4:00pm</td><td>Break</td><td>Break</td><td>Break</td><td>Break</td></tr>
<tr><td>4:00pm-6:00pm</td><td></td><td>SeaPerch</td><td>SeaPerch</td><td>SeaPerch</td><td>Brainstorm</td></tr>
<tr><td>Evening</td><td colspan="7">Free</td></tr>
</table>

Time	July 4	July 5	July 6	July 7	July 8	July 9	July 10
8:00am-9:45am		Registration, Logistics	Tascón	**Free**	Carreño	Wrap Up 2	
9:45am-10:00am			Break		Break	Break	
10:00am-12:00pm		Woosley	Ordoñez	**Shipyard Tour (Cotecmar) Depart Hotel at 9:30 am**	Chyba	SeaPerch	**CTG Hotel to Airpot Transportation**
12:00pm-2:00pm	**Free**	**Lunch**			**Lunch**		
2:00pm-3:45pm		Eustice	Neu		Cooper & Nelson	Contreras ENAP vessel demo & SeaPerch Challenge	
3:45pm-4:00pm		Break	Break		Break		
4:00pm-6:00pm	**Barbecue**	**Free**	SeaPerch	**Free**	*CFD Presentations:* Ubach, Jones, Bloxom, Coe; Mod: Martin		
Evening			**Night Tour (Optional)**		**Free**		

*Rader presentation moved to July 8

funding. This K-12 outreach activity is designed to introduce students to fundamental concepts in engineering and naval architecture ranging from teamwork to Archimedes' principle. By having PASI participants build SeaPerch vehicles, the PASI served the dual purpose of essentially becoming an international SeaPerch teacher training session. This emphasis on outreach was a core component of the PASI with talks scheduled to focus on teaching with underwater vehicles.

In addition to the technical lecturers and presentations, available online at the PASI website: http://www.pasi.aoe.vt.edu, and SeaPerch activities, highlights of the program included a river trip on a buoy tending vessel along the Rio Magdalena and a tour of COTECMAR's shipyard. This allowed participants to have strong exposure to the specific needs and interests of the Colombian commercial and military naval sector. Additional social activities included a scenic tour between Barranquilla and Cartagena with a beachside stop for fish, swimming, and soccer, along the Caribbean at Caño Dulce and experiencing the mud volcano Volcán del Totumo, a holiday barbeque at the Colombian Naval Officers' Club hosted by COTECMAR, an evening chiva tour of Cartagena, and a free-day to sightsee. A brief pictorial summary is given in Fig. 2.

During the institute, the usage of surface and semi-submersible small vessels for drug trafficking from

Fig. 2a. Participants and lecturers aboard a buoy tending vessel on the Rio Magdalena

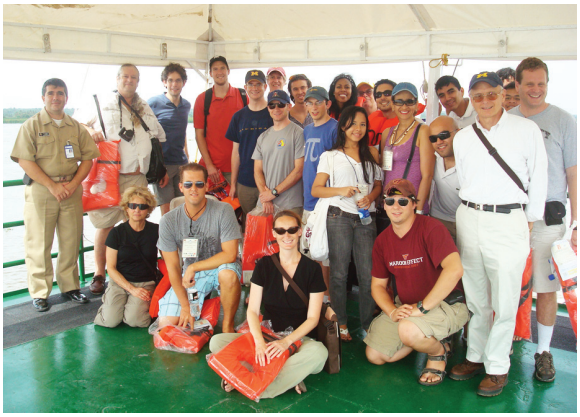

Fig. 2b. The victors from the PASI SeaPerch competition

South American countries to Central and North America was discussed. Thanks to COTECMAR and the Colombian Navy's Coast Guard Station in Cartagena, the participants were briefed on the challenges of this type of activity and the successful interdiction operations of recent years. PASI attendees had the opportunity to take a close look at four indicted vessels stationed in Cartagena's Coast Guard Station.

Fig. 2c. Participants' view of buoy tending

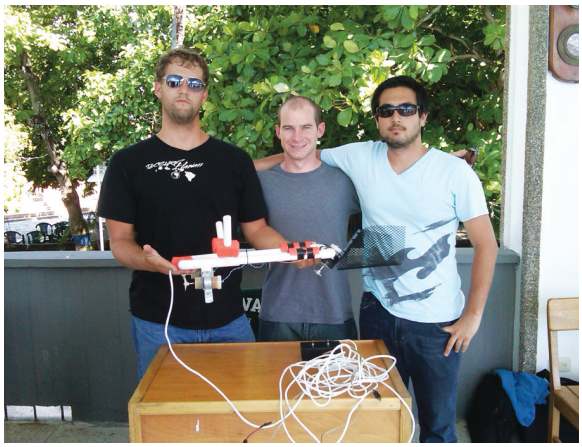

Fig. 2d. PASI participants studying density and viscosity in Volcán del Totumo outside Barranquilla, Colombia

Fig. 2e. PASI participants and lecturers at the Cotecmar Mamonal facility

Fig. 2f. Colombian Coast Guard captured semi-submersible

Findings

While full technical details of the presentations are available on the PASI website at http://www.pasi.aoe.vt.edu, specific findings included highlighting the interplay between technologies developed for unmanned vehicles as applicable to manned vehicles, sensors, development of traditional and non-traditional computational fluid dynamics approaches for design and control, and the importance of reaching the next generation of young engineers via exciting hands-on outreach activities.

Participant and Lecture Feedback

Feedback from the participants and lecturers of the PASI was needed in order to evaluate the effectiveness of the program. This feedback was collect via a questionnaire-styled survey given to participants and lecturers at the beginning and conclusion of the program. The pre-survey was designed to gather information on demographics, as well as determining what the expectations of the participants and lecturers were before starting the program. The post-survey is designed to see if those expectations were met and if the mission of the PASI program was accomplished. Both surveys were administered in English and Spanish and the format of both surveys is given in Appendices A and B.

Demographics

The PASI program saw a diverse blend of lecturers and participants in terms of citizenship, location of work, and academic level. The demographic distribution of citizenship of the lecturers and participants completing the pre-survey is illustrated in Fig. 3(a), demographic distribution of location of work of the lecturers and participants completing the pre-survey is illustrated in Fig. 3(b), and the academic level of the lecturers and participants completing the pre-survey is illustrated in Fig. 3(c).

Fig. 3a. Pre-survey "In what country do you primarily hold citizenship?"

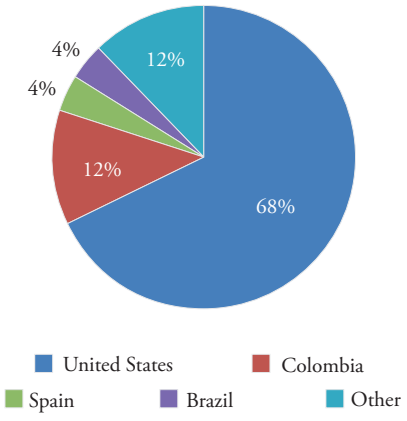

Fig. 3b. Pre-survey "In what country do you primarily works?"

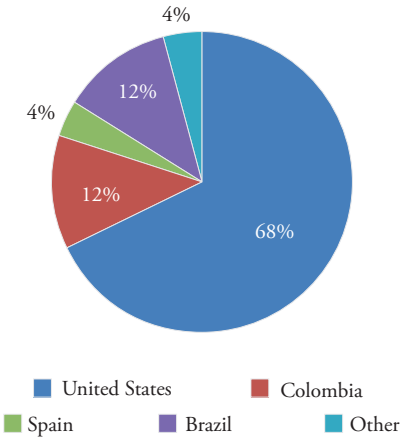

Fig. 3c. Pre-survey "What is your academy level?"

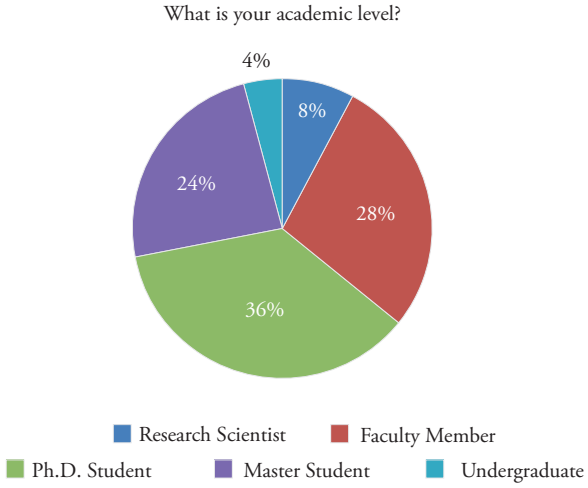

Program evaluation

Based on the pre-program survey, expectations of the lecturers and participants ranged from a desire to learn more about the technologies at hand and on-going research in the field to networking and a seeking to learn more about Colombian culture and foreign engineering methods.In response to the question "What do you expect to gain from participating in PASI," answers included:

> "Meet new people. Exchange ideas. Learn something new. Get exposure for my work. See a new country/culture."—*US faculty member*

"Learn about Colombia and manned & unmanned vehicles."—*US masters student*

"Learn about state of the art marine dynamics and controls. Meet people working in the field. Find ideas for collaborative projects in the topic of the PASI"—*Colombian PhD student*

"1) Relationships with colleagues from domestic and international universities who have similar or complementary research interests.
2) A better understanding of the Colombian Navy's challenges, particularly wrt riverine operations. (Riverine USVs are a current research interest.)"—*US faculty member*

"Compartir experiencias y advances en los temas centrales del PASI. Conocer colegas de otros paises y generar redes"—*Masters student studying in Brazil*

Participants and lecturers were asked in the post-survey questionnaire whether or not their expectations from the beginning of the program were met, the results of which are presented in Fig. 4. Based on the responses they gave prior to the start of the program, participants and lecturers could indicate whether they strongly agreed, agreed, felt neutral, disagreed, or strongly disagreed that their expectations of the PASI event were met. From the results, it is apparent that a vast majority of respondents felt that what they sought to gain from PASI was achieved.

An effective method to assess whether the program accomplished its mission was to directly ask the students and lecturers in attendance. Two of the main goals of the PASI program involvedisseminating scientific and engineering knowledge as well as uniting researchers from the Americas to stimulate cooperation and training (NSF, 2010). Figs. 5(a) and 5(b) show the degree to which the respondents felt this was accomplished.

Fig. 4. Post-survey Respondents' Feedback on Expectations

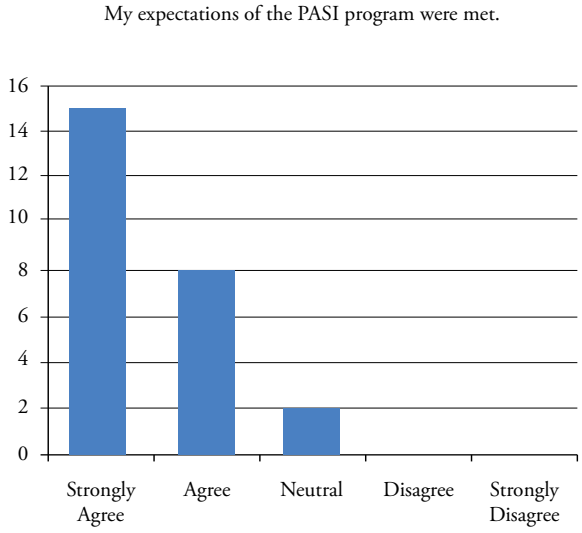

Fig. 5a. Post-Survey Respondents' Assessment of Knowledge Dispersal

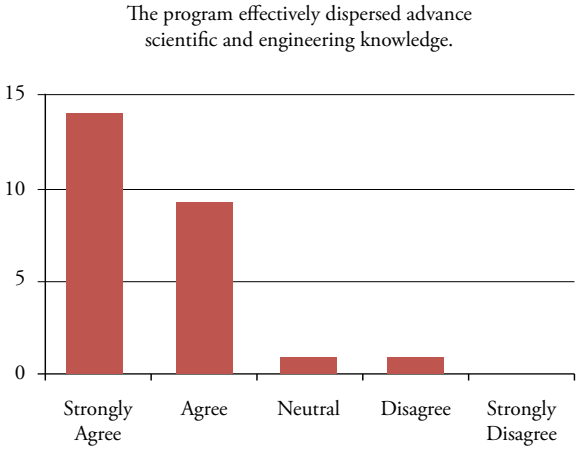

Fig. 5b. Post-Survey Respondents' Assessment of Training and Cooperation Stimulation

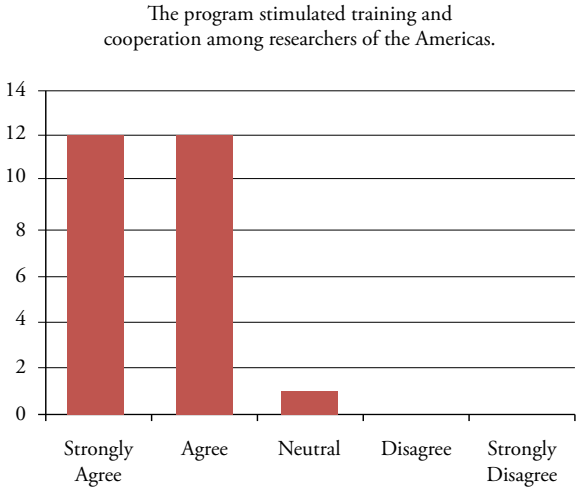

As indicated, an overwhelming majority of the respondents either agreed or strongly agreed that the goals of PASI were met, speaking to the overall effectiveness of the program.

In addition, participants and lecturers were also asked to evaluate the quality of the conference speakers. Fig. 6 shows that all respondents felt the instructors were either excellent or good.

Fig. 6. Post-Survey Respondents' Opinion of Speaker and Instructor Quality.

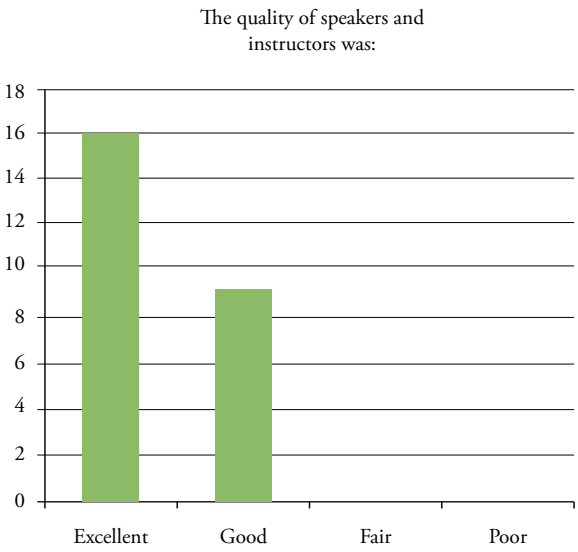

Program evaluation

On the post-survey, lecturers and participants were also asked to suggest areas of improvement for future PASI-like gatherings of scientists and engineers. Many respondents expressed that they were happy with the way the program was executed, though some made suggestions to reduce the overall length of the program.

There were also some respondents that expressed a desire to have more group work present during the sessions. Group work in the PASI as scheduled was limited to end-of-week wrap up sessions and the SeaPerch hands-on outreach activity. While long lunches were scheduled deliberately to allow time for individual interaction, structuring this into 'active learning' exercises in each session certainly makes sense in the context of learning theory, is highly feasible, and would be a welcome addition to any PASI program.

In response to the question "Do you have any suggestions for improvements of the program?" answers included:

> "Shorter lectures and more group work. For example, each lecturer could provide short (~30 minutes) activity for participants to work on after each lecture. Participants would be encouraged to work with different groups every day."—*US PhD student.*

> "The mix of technical and personal interaction is ideal to encourage collaboration among the participants"—*US faculty member.*

> "Very effective as is. My expectations were different but then I realized how naive I was in these, and learned a lot. Was a significant 'eye opener' for me regarding issues, the military situation, and required technologies well beyond my previous assumptions. Moreover, meeting the various parties, NAVY, CG, etc, face-face in their facilities was far more effective than meeting them in the US.
> **Improvements:** possibly some side-bar meetings + time with principles to discuss business; or not…*i.e.* prior development of gaps & issues (CUT TO CHASE) and technologies on the other side; bring together in a form of applicability. Prior to program, identify and initiate POCs state-side for possible business + funding routes=do this up front prior to travel so 'follow-up' is clear and pre-initiated. Follow-up is usually what fails to happen with these conferences."—*US research scientist.*

> "The overall program was good and there was a variety of different marine vehicle presentations. It was well organized but perhaps a little smaller of an event than I expected. The Colombian hosts did a great job at making the participants comfortable and entertained. More students would be

nice because we have the most to gain from this experience. Overall, I had a fantastic trip!"—*US masters student*.

Acknowledgments

The Pan-American Advanced Studies Institute on Dynamics and Control of Manned and Unmanned Marine Vehicles was generously supported by the United States National Science Foundation (NSF) and Department of Energy (DOE) under grant number OISE-0921820 and the oversight of NSF program officer Dr. Harold Stolberg. Additionally, support for the PASI was provided by Universidad del Norte and Escuela Naval "Almirante Padilla," the two host organizations for the PASI, Virginia Tech including the Virginia Center for Autonomous Systems (VaCAS) and the Aerospace and Ocean Engineering (AOE) Department, Cotecmar, DIMAR, the Office of Naval Research (ONR) and the Office of Naval Research—Global (ONRG), the Society of Naval Architects and Marine Engineers (SNAME) and Maritime Reporter.

The authors are also tremendously grateful to everyone who assisted on the organizing committees and in the nitty-gritty making the program happen details including Maria Claudia Durango Dickson (UniNorte), Ely Acosta (UniNorte), Rosa Avalos (VT), Jon Couch (VT), CMDR Oscar Tascón (Cotecmar), CAPT Jorge Carreño (Cotecmar), Fernando Delgado (Cotecmar), Carlos Mojica (Cotecmar), Luis Aranibar (Cotecmar), Jimmy Saravia (Cotecmar), CMDR Fabio Zapata (Escuela Naval), Germán García (Escuela Naval), ADM Luis Ordoñez (Escuela Naval), Marcelo Santos Neves (UFRJ) and Armin Troesch (UM). And last, but certainly not least, the authors wish to thank the wonderful lecturers and participants, without whom this PASI never would have happened.

References

AUVSI, *"Association for Unmanned Vehicle Systems International,"* http://www.auvsi.org/AUVSI/AUVSI/Home/, accessed July 2010.

NSF, *"Pan-American Advanced Studies Institutes Program (PASI),"* http://www.nsf.gov/pubs/2010/nsf10517/nsf10517.htm, accessed August 2010.

SNAME, *"The official site of SeaPerch,"* http://www.seaperch.org, accessed: July, 2010.

Appendix A: Pre-survey

VirginiaTech

English

1. In what country do you primarily hold citizenship?
a) Argentina
b) Brazil
c) Colombia
d) Spain
e) United States
f) Other

2. In what country do you primarily work?
a) Argentina
b) Brazil
c) Colombia
d) Spain
e) United States
f) Other

3. What is your gender?
a) Male
b) Female

4. What is your academic level?
a) Ph.D Student
b) Masters Student
c) Undergrad Student
d) Faculty Member
e) Research Scientist

5. What do you expect to gain from participating in PASI?

_____
_____
_____
_____
_____

Español

1. ¿En qué país tiene ciudadanía?
a) Argentina
b) Brasil
c) Colombia
d) España
e) Estados Unidos
f) Otros

2. ¿En qué país trabaja primariamente?
a) Argentina
b) Brasil
c) Colombia
d) España
e) Estados Unidos
f) Otros

3. ¿Cuál es su género?
a) Masculino
b) Femenino

4. ¿Cuál es su nivel académico?
a) Estudiante de Ph.D.
b) Estudiante de Maestría
c) Estudiante Universitario
d) Miembro de facultad
e) Científico de investigaciones

5. ¿Qué espera obtener al participar en PASI?

_____
_____
_____
_____
_____

Appendix B: Post-survey (English)

VirginiaTech

English

1. In what country do you primarily hold citizenship?
a) Argentina
b) Brazil
c) Colombia
d) Spain
e) United States
f) Other

2. In what country do you primarily work?
a) Argentina
b) Brazil
c) Colombia
d) Spain
e) United States
f) Other

3. What is your gender?
a) Male
b) Female

4. What is your academic level?
a) Ph.D Student
b) Masters Student
c) Undergrad Student
d) Faculty Member
e) Research Scientist

5. My expectations of the PASI program were met.
a) Strongly Disagree
b) Disagree
c) Neutral
d) Agree
e) Strongly Agree

6. The program effectively dispersed advanced scientific and engineering knowledge.
a) Strongly Disagree
b) Disagree
c) Neutral
d) Agree
e) Strongly Agree

7. The program stimulated training and cooperation among researchers of the Americas.
a) Strongly Disagree
b) Disagree
c) Neutral
d) Agree
e) Strongly Agree

8. The quality of speakers and instructors was:
a) Excellent
b) Good
c) Fair
d) Poor

9. The quality of the facilities and equipment used in Barranquilla was:
a) Excellent
b) Good
c) Fair
d) Poor

10. The quality of the facilities and equipment used in Cartagena was:
a) Excellent
b) Good
c) Fair
d) Poor

11. Do you have any suggestions for improvements of the program? (fill in below)

_____
_____
_____
_____
_____

Appendix B: Post-survey (Español)

VirginiaTech

Español

1. ¿En qué país tiene ciudadanía?
a) Argentina
b) Brasil
c) Colombia
d) España
e) Estados Unidos
f) Otros

2. ¿En qué país primariamente trabaja?
a) Argentina
b) Brasil
c) Colombia
d) España
e) Estados Unidos
f) Otros

3. ¿Cuál es su género?
a) Masculino
b) Femenino

4. ¿Cuál es su nivel académico?
a) Estudiante de Ph.D.
b) Estudiante de Maestría
c) Estudiante Universitario
d) Miembro de facultad
e) Científico de investigaciones

5. Mis expectativas del programa PASI se cumplieron
a) Totalmente en desacuerdo
b) En desacuerdo
c) Neutral
d) De acuerdo
e) Totalmente de acuerdo

6. El programa difundió efectivamente conocimientos científicos y de ingeniería avanzados.
a) Totalmente en desacuerdo
b) En desacuerdo
c) Neutral
d) De acuerdo
e) Totalmente de acuerdo

7. El programa estimuló la preparación y cooperación de investigadores de las américas.
a) Totalmente en desacuerdo
b) En desacuerdo
c) Neutral
d) De acuerdo
e) Totalmente de acuerdo

8. La calidad de los oradores e instructores fue:
a) Excelente
b) Buena
c) Regular
d) Mala

9. La calidad de las instalaciones y equipo usado en Barranquilla fue:
a) Excelente
b) Buena
c) Regular
d) Mala

10. La calidad de las instalaciones y equipo en Cartagena fue:
a) Excelente
b) Buena
c) Regular
d) Mala

11. ¿Tiene algunas sugerencias para poder mejorar el programa? (Llene abajo)

_____
_____
_____
_____
_____

SPH Boundary Deficiency Correction for Improved Boundary Conditions at Deformable Surfaces

SPH Corrección de la deficienccia de límites para la mejora de condiciones de contornos en superficies deformables

Van Jones[1]
Qing Yang[2]
Leigh McCue-Weil[3]

Abstract

Smoothed particle hydrodynamics (SPH) is a meshless, Lagrangian CFD method. SPH often utilizes static virtual particles to correct for integral deficiencies that occur near boundaries. These virtual particles, while useful in most cases, can be difficult to implement for objects which experience large deformations. As an alternative to virtual particles, a repulsive force algorithm is presented which loosely emulates the presence of virtual particles in the SPH momentum equation.

Key words: Smoothed Particle Hydrodynamics, SPH, SPH Boundary Condition.

Resumen

La Hidrodinámica de Partículas Suavizadas (Smoothed Particle Hydrodynamics, SPH) es un método CFD Lagrangiano sin malla (Mecánica de Fluidos Computacional, CFD). El método SPH frecuentemente utiliza partículas estáticas virtuales para corregir las deficiencias integrales que ocurren cerca de las fronteras. Estas partículas virtuales, aunque son útiles en la mayoría de los casos, pueden ser difíciles de implementar para objetos que experimentan grandes deformaciones. Como alternativa a las partículas virtuales, se presenta un algoritmo de fuerza repulsiva que emula indirectamente la presencia de las partículas virtuales en la ecuación de momento del método SPH.

Palabras claves: Hidrodinámica de Partículas Suavizadas, Condiciones de frontera de SPH.

Date received: May 20th, 2010. - *Fecha de recepción: 20 de Mayo de 2010.*
Date Accepted: July 6, 2010. - *Fecha de aceptación: 6 de Julio de 2010.*

[1] Virginia Tech. e-mail: cerchio@vt.edu
[2] Virginia Tech. e-mail: royyang@vt.edu
[3] Virginia Tech. e-mail: mccue@vt.edu

Overview of Smoothed Particle Hydrodynamics

Smoothed particle hydrodynamics was first developed for applications in astrodynamics [1][2]. SPH was later adapted to fluid dynamics due to its ability to efficiently simulate complex free surface flows. It is based on the ability of a kernel function to approximate a field value at a point by integrating over surrounding field values. A kernel function is a finite area approximation of the Dirac delta function. The SPH approximation can be seen by first considering the integration result of the product of a field and the Dirac delta function (Eqn 1a). This integration exactly yields the field value at the location of the Dirac delta function. By replacing the discontinuous Dirac delta with a kernel function possessing similar properties (but defined over a finite area) a useful approximation of field functions can be obtained (Eqn 1b). This formula can then be discretized to obtain an equation applicable to Lagrangian particle dynamics (Eqn 1c). In the discretization, W_{ij} is the value of the kernel function between a subject particle (i) and an influencing particle (j) with A_j as the area or volume associated with the influencing particle [8].

$$f(x) = \int_x \delta\,(x - x')\, f(x')\, dx' \tag{1a}$$

$$f(x) \approx \int_\Omega W(x - x', h)\, f(x')\, dx' \tag{1b}$$

$$f_{ii} \approx \sum_\Omega W_j\, f_j\, A_j \tag{1c}$$

The integration limits for Eqn 1a can be infinite with identical results. However, because the integration product is zero everywhere except at $x' = x$, the integration limits can be reduced to encompass only the point x. Similarly, most kernel functions with compact support domain are defined as zero beyond a set radius. It follows that the integration/summation region for Eqns 1b and 1c need only encompass the region in which the kernel function is defined to be non-zero.

A classic kernel function, described by Monaghan and Lattanzio, is the Cubic-spline function (Fig. 1) [12].

Fig. 1. Cubic Spline Smoothing Function and Derivative, 2D Visualization

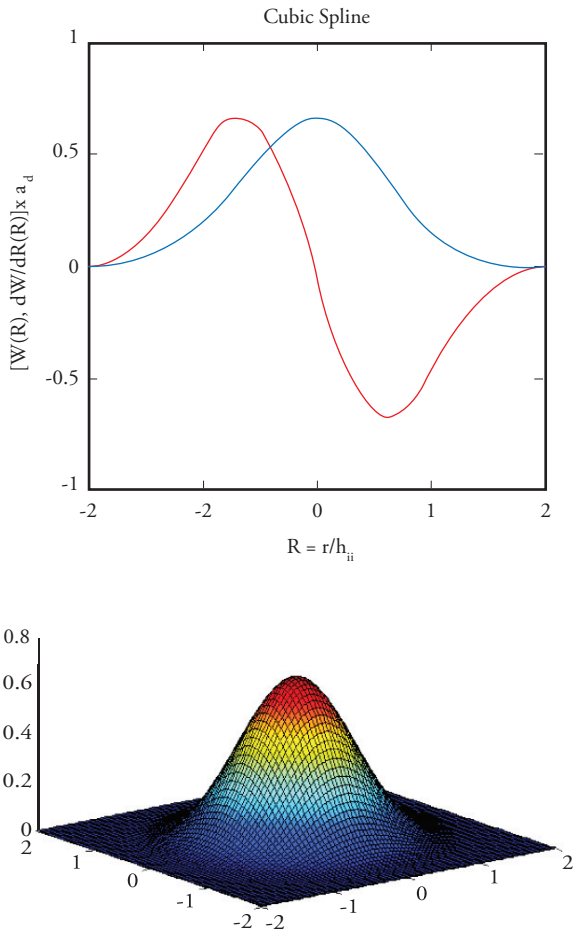

The Cubic-spline kernel function is defined as non-zero for all $r < 2h$ (where h is a scaling parameter typically based on particle mass). It follows that the integration domain Ω of equation 1b is the region within a radius of $2h$ of the point x. Similarly, for equation 1c the support domain particles (Ω) consist of all particles within $2h$ of the subject particle i as illustrated in Fig. 2.

The SPH method can be applied to fluid dynamics in a number of ways. A common technique to adapt SPH to fluid dynamics is Weakly Compressible Smoothed Particle Hydrodynamics (WCSPH). In WCSPH, fluids typically considered nearly incompressible are allowed a small degree of compressibility. This yields a finite speed of sound

Fig. 2. SPH Particle Support Domain

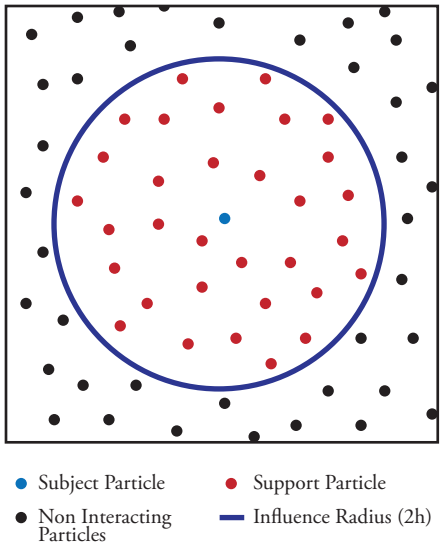

for the fluid and changes the characteristic of the governing equations to allow for uncoupled solving of particle properties. Particle pressures are derived from an equation of state. The parameters of the equation of state determine the numerical speed of sound in that medium. The Tait Equation (Eqn 2) is a commonly used equation of state for water simulations [13].

$$p_i = \beta\left(\frac{\rho}{\rho_0} - 1\right)^{\gamma} + p_0 \quad \left(where\ \beta = \frac{v_{sound}\,\rho_0}{\gamma}\right) \tag{2}$$

Two common methods exist to calculate SPH particle density, these are the summation and continuity density formulations. The summation density formulation directly determines density by summing the kernel-weighted densities of all support domain particles (Eqn 3a). Substituting the definition of density (Eqn 3b) into Eqn 3a yields Eqn 3c [8] and tranforms the formula into a mass summation over an implied volume (the kernel function has units of inverse volume).

$$\rho_i = \sum_{j=1}^{N} W_{ij}\,\rho_j\,A_j \tag{3a}$$

$$\rho_j = \frac{m_j}{A_j} \tag{3b}$$

$$\rho_i = \sum_{j=1}^{N} W_{ij}\,m_j \tag{3c}$$

The continuity density formulation instead calculates the velocity divergence for each particle. Because the velocity divergence of a fluid is equivalent to the time rate-of-change of density this value can be integrated over time to obtain density change. The corresponding particle discretized formula for the continuity density formulation is shown in equation 4 [8].

$$\frac{D\rho_i}{Dt} = \sum_{j=1}^{N} m_{ji} v_j \frac{\partial W_{ij}}{\partial x_{ij}} \quad (where\ v_{ij} \equiv \vec{v}_i - \vec{v}_j) \tag{4}$$

Particle acceleration is determined from the stress tensor for each particle ($\sigma^{\alpha\beta}_j$). The stress tensor can be separated into translational (pressure) and viscous shear stresses. Shear stress can be approximated as the product of fluid's dynamic viscosity (μ) and strain rate tensor ($\epsilon^{\alpha\beta}_j$). For inviscid cases (μ=0), the particle discretized momentum equation reduces to a simple pressure-force summation. Equation 5 shows the particle discretized SPH momentum equation [8].

$$\begin{aligned}\frac{Dv_i}{Dt} &= \sum_{j=1}^{N} m_j\left(\frac{\sigma^{\alpha\beta}_i}{\rho_i^2} + \frac{\sigma^{\alpha\beta}_j}{\rho_j^2}\right)\frac{\partial W_{ij}}{\partial x_{ij}} \\ &= -\sum_{j=1}^{N} m_j\left(\frac{p_i}{\rho_i^2} + \frac{p_j}{\rho_j^2}\right)\frac{\partial W_{ij}}{\partial x_{ij}} \\ &\quad + \sum_{j=1}^{N} m_j\left(\frac{\mu_i \epsilon^{\alpha\beta}_i}{\rho_i^2} + \frac{\mu_i \epsilon^{\alpha\beta}_j}{\rho_j^2}\right)\frac{\partial W_{ij}}{\partial x_{ij}}\end{aligned} \tag{5}$$

where

$$\epsilon^{\alpha\beta}_i = \sum_{j=1}^{N}\frac{m_j}{\rho_j} v^{\beta}_{ji}\frac{\partial W_{ij}}{\partial x^{\alpha}_i} + \sum_{j=1}^{N}\frac{m_j}{\rho_j} v^{\alpha}_{ji}\frac{\partial W_{ij}}{\partial x^{\beta}_i}$$

$$-\left(\frac{2}{3}\sum_{j=1}^{N}\frac{m_j}{\rho_j} v_{ij}\cdot\nabla W_{ij}\right)\delta^{\alpha\beta}$$

SPH Boundary Behavior

Assuming uniformly distributed particles in an unbounded region, the SPH particle discretized governing equations approach the Navier Stokes governing equations as smoothing length approaches zero. The unbounded assumption is required to satisfy that fluid field values exist at all points within a particle's support domain. When a particle's support domain has an insufficient number of particles to adequately approximate the fluid field values within its support radius it is said to be integral or boundary deficient. One way in which this can occur is if particle smoothing radius is set to a small value such that very few particles fall within a support radius, in this case the SPH governing equations will yield poor approximations of field functions. Because of this smoothing radius is typically empirically related to particle mass and density such that an acceptable influence radius is maintained. A second more complicated manner in which integral deficiency can occur is observable when a particle is within close proximity to a fluid boundary. This situation is shown in Figure 3, which plots particle acceleration of a finite 1D constant pressure fluid. While there exists no pressure gradient in the fluid, near-boundary particles exhibit a non-zero acceleration or boundary deficiency in acceleration.

This behavior is desirable at free surfaces for single-phase simulations as the boundary deficiency behaves identically to a zero gauge pressure fluid. However, boundary deficiency leads to difficulties at fluid-object boundaries. Relatively robust boundary conditions can be created by using repulsion forces based on spatial proximity (see [3][4][5]). However, because of the lack of a pressure term to correct for boundary deficiency, proximity-based repulsion boundaries tend to yield a nonphysical varying fluid particle to wall spacing at equilibrium. Typically this boundary deficiency is addressed by populating boundary regions with virtual particles whose properties are either fixed or derived from nearby fluid particles (see [6][7]). Robust boundary conditions which do not exhibit varying particle wall separation distance can be obtained by combining a spatial repulsive boundary with virtual particles [8][9][10]. However, for cases in which large boundary deformations can occur, virtual particle placement can become problematic due to virtual particle clumping. Clumping is a particle artifact in which particle spacing becomes skewed such that a directional spacing bias is present. This can result in an integral deficiency or surplus which increases the error of calculated field values. Fig. 4 shows an example of fixed virtual particle clumping due to boundary deformation. Visible in Fig. 4 is clumping resultant from deforming a boundary (shown in red). In the convex deformation case, near-boundary fluid particles experience a virtual particle integral surplus. Likewise, concave deformations lead to an integral deficiency.

Fig. 3. Boundary Deficiency in Acceleration (influence radius = 1)

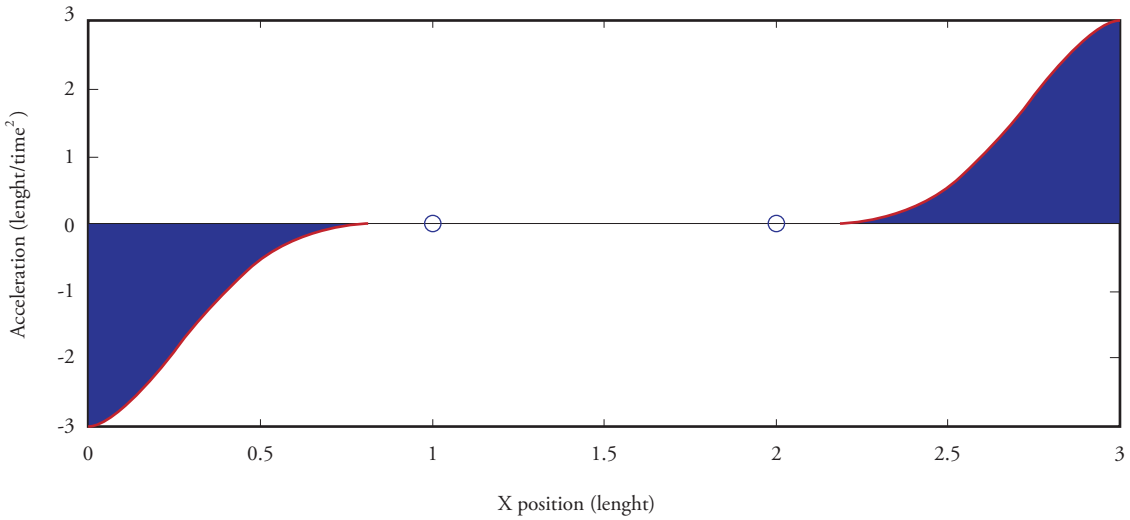

Fig. 4. Clumping of Virtual Particles due to Deformation

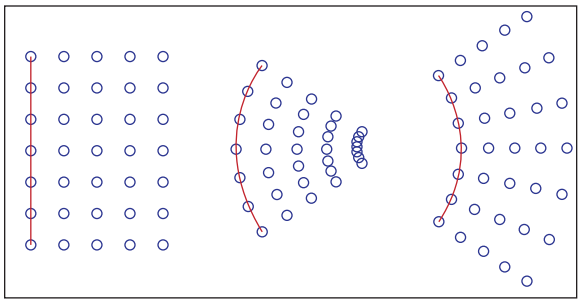

It is therefore desirable to provide an alternative to virtual particles for boundary deficiency correction of highly deformable objects. While various correction methods exist which achieve similar results, they are often computationally expensive. Feldman and Bonet developed one such method to correct boundary deficiency for straight and corner boundaries by generating a curve fit to boundary deficiency accelerations [11].

While the goal is to achieve a boundary deficiency correction for arbitrary boundaries, it is advantageous to first consider the simple case of a 1-dimensional boundary. By observation of the boundary deficiency of a one dimensional fluid as in Fig. 3, it apparent that the boundary deficiency is similar in shape to the smoothing function. Analyzing equation 5 acting at a boundary and assuming constant pressure, density, and mass, the momentum equation can be reduced as shown in equation 6.

$$m_j\left(\frac{p_i}{\rho_i^2}+\frac{p_j}{\rho_j^2}\right)\sum_{j=1}^{N}\frac{\partial W_{ij}}{\partial x_{ij}}=\frac{2\,m\,p}{\rho^2}\sum_{j=1}^{N}\frac{\partial W_{ij}}{\partial x_{ij}} \qquad (6)$$

$$=\frac{2\,A\,p}{\rho^2}\,W_{ij}\boxtimes\ CW_{ij}$$

Equation 6 shows that the acceleration boundary deficiency is proportional to the total area of the deficiency as well as fluid pressure. Because cases of interest typically involve non-constant pressures equation 6 is not strictly suitable for use as a boundary correction. However proportionality to the kernel function for boundary deficiency can stil be observed even in cases in which a pressure gradient is present. Fig. 5 illustrates one such case. Shown in Fig. 5 is the vertical acceleration of a unity density fluid influenced by a downward body acceleration of unity magnitude.

Fig. 5. Vertical Water Column Boundary Deficiency (influence radius=1)

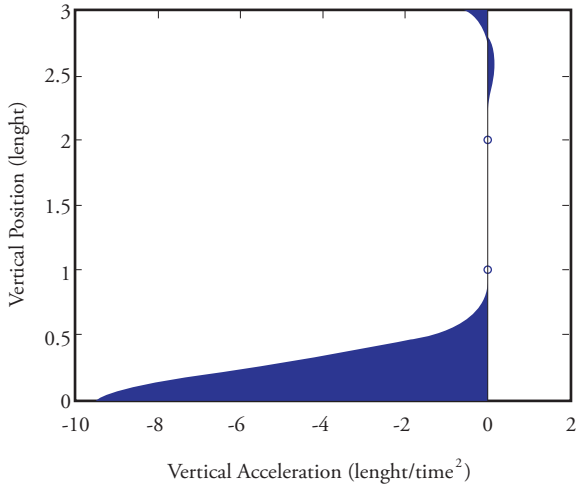

The pressure at the top of the water column is zero (gauge pressure), with pressure in the fluid varying as $dp/dz=-\rho g$. The boundary deficiency in acceleration at the bottom of the water column still strongly correlates to the kernel function even in the presence of a pressure gradient. It is interesting to note that a boundary deficiency exists not only at the bottom boundary but also at the free surface. However, the low magnitude boundary deficiency at the free surface does not introduce substantial error as it typically results in only minor particle clumping.

Acceleration Boundary Deficiency Correction

While an exact acceleration boundary deficiency correction could be gained by discerning the pressure gradient normal to a surface and analyzing the geometry of the deficiency, such an approach would increase computational complexity. Instead a simple -if inexact- correction is suggested in which the pressure is assumed to be nearly constant over the scale of the smoothing length. Then by assuming a known boundary acceleration, the relative fluid-boundary acceleration in the absence of boundary forces can be calculated. If this relative acceleration is assumed to be the result of a boundary

deficiency then it can be corrected by applying a repulsive acceleration distributed as CW_{ij} away from the boundary. Where C is determined by choosing a sample particle, determining the relative particleboundary normal acceleration and dividing by W_{ij} . To improve robustness it is advisable to average C over a small sample of near-boundary particles. This reduces correction error due to spurious pressure fluctuations. Equation 7 shows this one dimensional acceleration boundary deficiency correction with j representing a boundary particle index.

$$\frac{D\,v_i}{Dt}_{correction} = -\,C_j\,W_{ij} \tag{7}$$

where

$$C_j = \frac{D\,v_i}{Dt}_{uncorrected} / W_{ij}$$

The assumption that a boundary acceleration is known is suitable for fixed boundaries but requires an approximation when applied to freely moving boundaries. For objects with much greater density than the surrounding fluid, forward interpolation of acceleration is acceptable as object acceleration will change only slowly relative to the simulated timescales when acted on by fluid forces alone. However, as relative object-fluid density decreases, this approximation worsens. Further work is necessary to assess the impact of this assumption on low density object dynamic behavior.

While the correction presented in equation 7 is sufficient for one dimensional cases where a single boundary particle governs a boundary deficient region, extension to higher dimensions requires a blending of corrections from multiple boundary particles. An empirical weighting function to blend correction values for two dimensional cases is shown in equation 8. Fig. 6 shows a visualization of the resultant weights.

$$\frac{D\,v_i}{Dt}_{correction} = -\,C_j\,W_{ij}\,weight_{i,\,normalized} \tag{8}$$

$$weight_{ij,\,normalized} = \frac{weight_{ij}}{\sum_{\Omega'} weight_{ij}\cdot\hat{n}_i\cdot\hat{n}_j}$$

(where Ω' is the set of all boundary particles within $r_{influence}$ of particle i)

$$weight_{ij} = ActivationParameter^2 + (GlancingParameter^2 + \frac{1}{2}) \cdot DistanceParameter$$

$$ActivationParameter = \frac{spacing}{\|\vec{r}_{ij}\|}$$

(where *'spacing'* is the local boundary particle spacing)

$$GlancingParameter = \frac{\vec{r}_{ij}}{\|\vec{r}_{ij}\|}\cdot\hat{n}_{boundary}$$

$$DistanceParameter = 1 - \frac{\|\vec{r}_{ij}\|}{r_{influence}}$$

Fig. 6. 2D Boundary Correction Weight Blending Visualization (influence radius=0.775, boundary spacing=0.25, boundary radius of curvature=1)

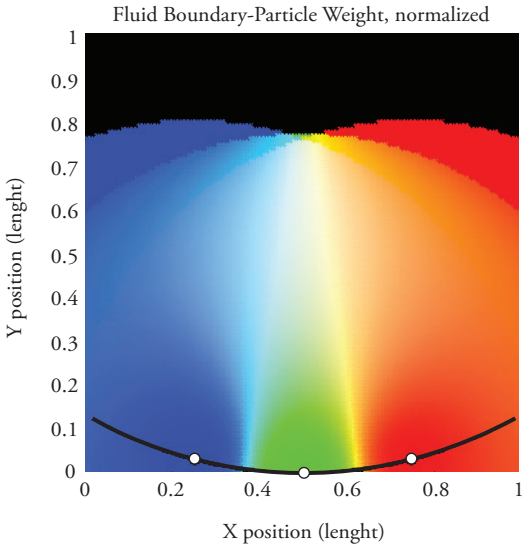

Fig. 6 illustrates the weighting scheme applied to simple concave and convex boundaries. The weights of the three boundary particles are shown by the blue, green, and red shades respectively.

The boundary deficiency correction is applied to two test cases (one with a rectangular boundary, one with an elliptical boundary) each with constant pressure fluid. Fig. 7 shows the rectangular tank case.

Fig. 6. 2D Boundary Correction Weight Blending Visualization (influence radius=0.775, boundary spacing=0.25, boundary radius of curvature=1)

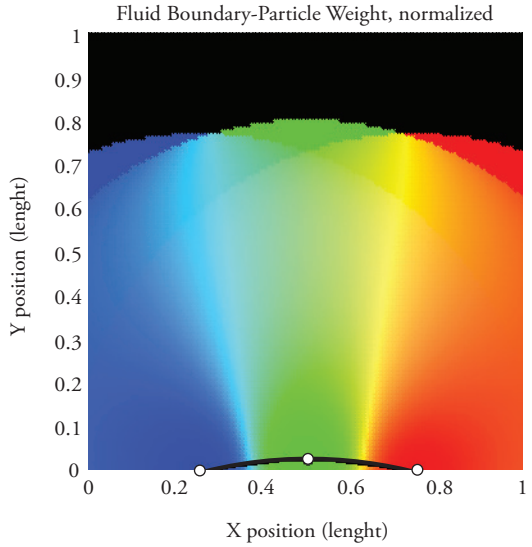

Fluid pressure is unity with density=1000. Particle influence radius set to 0.5. The unmodified acceleration field is presented on the left and the corrected acceleration field is shown on the right. The normalized acceleration correction magnitude for each boundary particle is shown in blue, and is plotted against boundary particle index (the zeroth boundary particle is located in the lower left with subsequent indexes moving counterclockwise about the rectangular tank). Fig. 8 shows the elliptical tank case with identical fluid and simulation parameters.

The four dips in correction acceleration visible in figure 7 (rectangular case) are due to the change in boundary deficiency due to the reduced volume of fluid present near the four tank corners. The correction slightly overcorrects the boundary deficiency in the sharp corners of the rectangular case. For the elliptical tank case, the acceleration present after boundary deficiency correction near the high curvature sides of the elliptic tank represents an undercorrection of the boundary deficiency and is likely a result of weighting function. Further refinement of the weighting function may reduce the error in the correction due to geometry. The low curvature and straight sections show good correction of acceleration boundary deficiency.

Because the correction presented emulates virtual particles, it alone is insufficient to act as a boundary

Fig. 7. Rectangular Tank Boundary Correction Test Case *(influence radius=0.5 spacing=$r_{influence}$/10)*

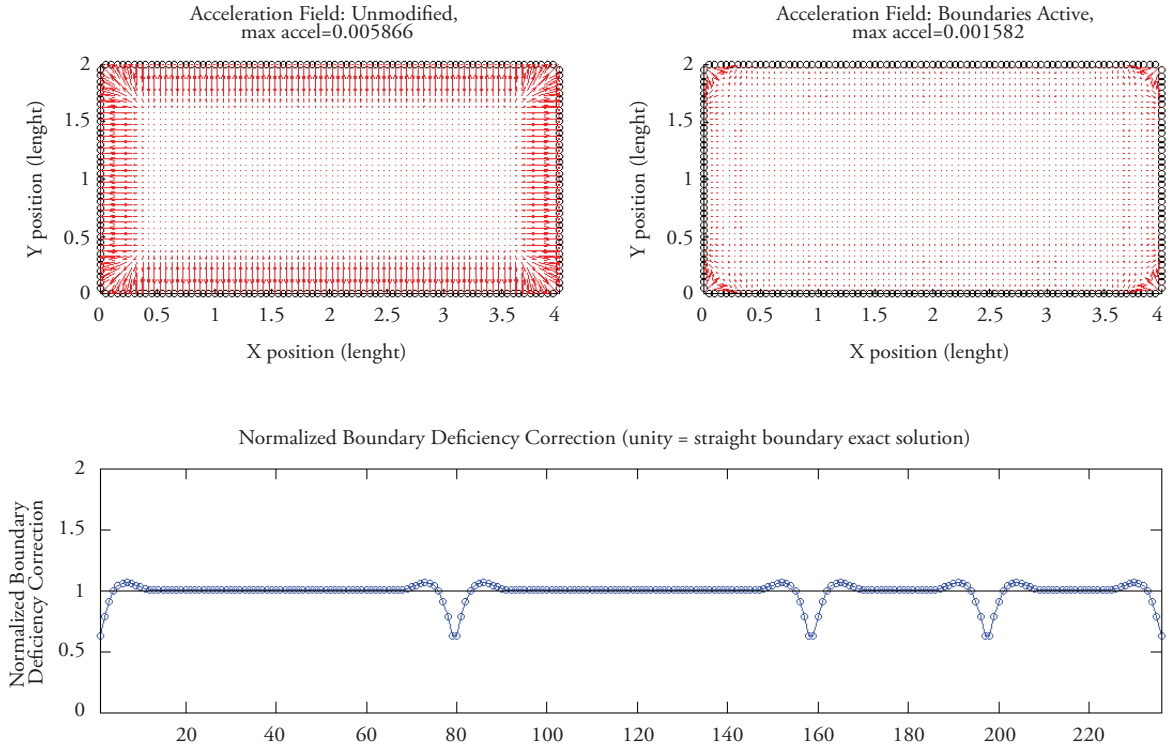

Fig. 8. Elliptical Tank Boundary Correction Test Case *(influence radius=0.5 spacing=$r_{influence}$/10)*

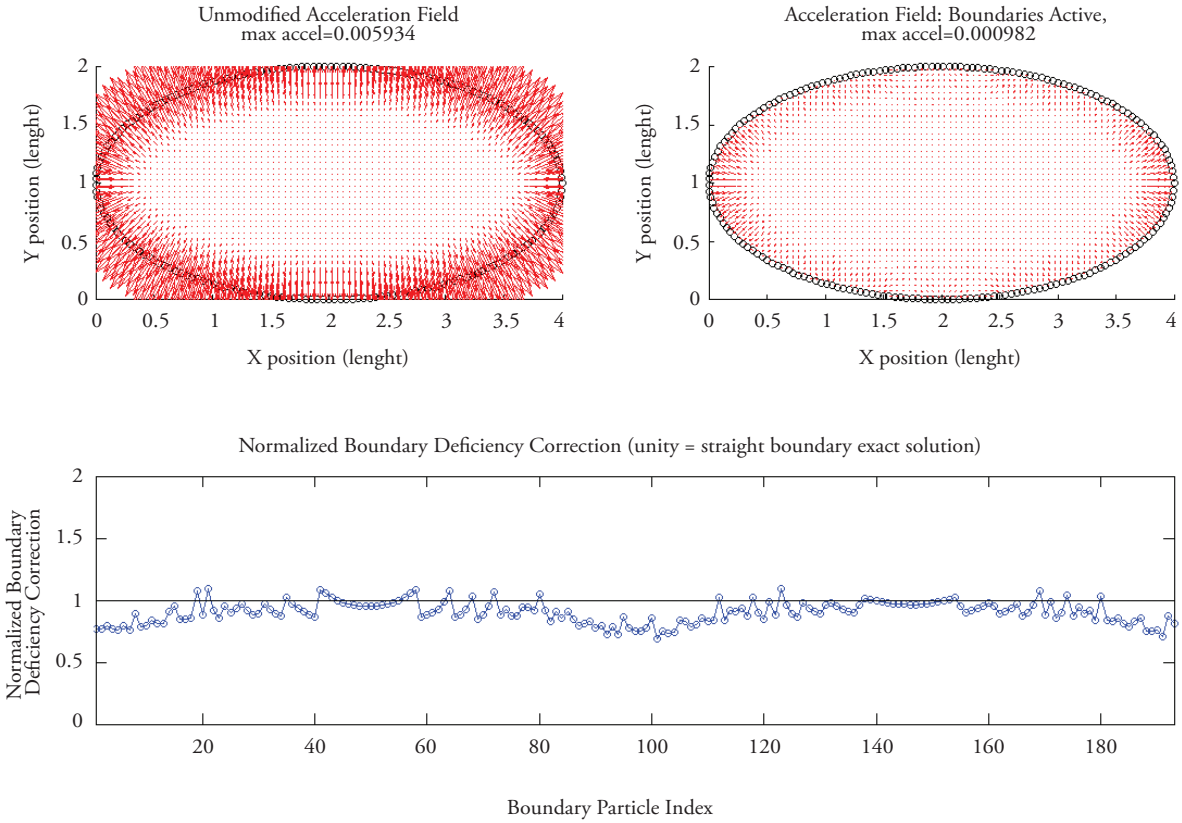

condition. A secondary repulsion force such as the spatial repulsion force developed by Monaghan in 2009 [5] is necessary to prevent fluid-boundary penetration. The presence of virtual particles or a boundary acceleration deficiency corrective force can improve the behavior of spatial repulsive boundary forces. This is especially noticeable in the transient behavior present at the start of most simulations involving spatial repulsive forces alone. By correcting the boundary acceleration deficiency immediately, near-boundary fluid particles do not have to re-orient to allow for a spatial change to correct the boundary repulsion force.

Similar boundary acceleration correction work performed by Feldman and Bonet [11] does not require an assumption of a known boundary acceleration, but instead determines an acceleration correction by calculating the fluid pressure gradient and assuming a known boundary geometry (straight or straight-corner). Further work is required to compare the relative performance of the two methods when applied to various cases.

Conclusions

Virtual particles are normally used to correct errors due to integral deficiencies that appear in the governing equations near boundaries. Virtual particle behavior for deformable objects can be difficult to implement due to particle clumping after deformation. A simple repulsive correction which loosely emulates the presence of virtual particles in the momentum equation has been derived. An empirical weighting function to extend the theoretical boundary correction to higher dimension cases has been presented. Results obtained by applying the boundary correction to two constant pressure test cases were presented. The method yields good correction of acceleration boundary deficiency in regions of low curvature

but tends to slightly overcorrect at sharp corners and undercorrect near regions with high curvature.

Acknowledgments

The authors would like to express their gratitude to Dr. Pat Purtell and Ms. Kelly Cooper at the Office of Naval Research for their sponsorship of this work under grant numbers N00014-08-1-0695, N00014-10-1-0398, and N00014-07-1-0833.

References

[1] LUCY L. B. (1977), '*Numerical approach to testing in the fission hypothesis*' in Astronomical Journal, 82 pp. 1013:1024.

[2] GINGOLD R. A. AND MONAGHAN J. J. (1977), '*Smoothed Particle Hydrodynmics: Theory and Application to Non-spherical stars*' in Monthly Notices of the Royal Astronomical Society, 181:375-389.

[3] MONAGHAN J. J. (1994). '*Simulating free surface flow with SPH*' in Journal of Computational Physics, 110:399-406.

[4] MONAGHAN, J. J.; KOS, A.; ISSA, N.. (2003) *'Fluid Motion Generated by Impact'* in Journal of Waterway, Port, Coastal & Ocean Engineering, Nov. 2003, Vol. 129 Issue 6, pp. 250-259.

[5] MONAGHAN, J. J. AND KAJTAR, J.B. (2009) *'SPH particle boundary forces for arbitrary boundaries'* in Computer Physics Communications, 2009, 180:1811–1820.

[6] LIBERSKY L. D., PETSCHECK A. G., CARNEY T. C, HIPP J. R. AND ALLAHDADI F. A. (1993), *'High strain Lagrangian hydrodynamics-a three-dimensional SPH code for dynamic material response'* in Journal of Computational Physics, 109:67-75.

[7] RANDLES P.W., AND LIBERSKY L. D. (1996), *'Smoothed particle hydrodynamics some recent improvements and applications'* in Computer Methods in Applied Mechanics and Engineering, 138:375-408.

[8] LIU, G. R. AND LIU, M. B.(2003). Smoothed Particle Hydrodynamics – a meshfree particle method, Toh Tuck Link, World Scientific Publishing.

[9] LIU G. R. AND GU Y. T. (2001), *'A local radial point interpolation method (LR-PIM) for free vibration analyses of 2-D solids'*. Journal of Sound and Vibration, 246(1):29-46.

[10] LIU M. B., LIU G. R. AND LAM K. Y. (2002), *'Investigations into water mitigations using a meshless particle method'* in Shock Waves 12(3):181-195.

[11] FELDMAN J. AND BONET J. (2007) *'Dynamic refinement and boundary contact forces in SPH with applications in fluid flow problems'* in Int. J. Numer. Meth. Engng 2007; 72:295–324.

[12] MONAGHAN, J. J. AND LATTANZIO J. C. (1985) *'A refined particle method for astrophysical problems'* in Astronomy and Astrophysics, 149:135-143.

[13] P. G. TAIT, (1888) Physics and Chemistry of the Voyage of H.M.S. Challenger, Vol. 2, Part 4 HMSO, London.

Creating Bathymetric Maps Using AUVs in the Magdalena River

Creación de mapas batimétricos usando vehículos submarinos autónomos en el río Magdalena

Dr. Monique Chyba[1]
John Rader[2]
Michael Andoinian[3]

Abstract

The goal is to develop a guidance and navigation algorithm for an AUV to perform high resolution scanning of the constantly changing river bed of the Magdalena River, the main river of Colombia, from the river mouth to a distance of 10 Km upriver, which is considered to be the riskiest section to navigate. Using geometric control we design the required thrust for an under-actuated autonomous underwater vehicle to realize the desired mission.

Key words: River Survey, Autonomous Underwater Vehicle.

Resumen

El objetivo es desarrollar un algoritmo de orientación y navegación para un AUV (Autonomous Underwater Vehicle) para realizar el escaneado de alta resolución del cambiante lecho del río Magdalena, principal río de Colombia, desde su desembocadura hasta una distancia de 10 Km río arriba, que se considera la sección de mayor riesgo para navegar. Usando control geométrico se diseñó el empuje necesario para un vehículo submarino autónomo subactuado para realizar la misión deseada.

Palabras claves: Vehículo submarino autónomo.

Date received: May 20th, 2010. - *Fecha de recepción: 20 de Mayo de 2010.*
Date Accepted: July 6, 2010. - *Fecha de aceptación: 6 de Julio de 2010.*

[1] University of Hawaii at Manoa, Honolulu, HI. e-mail: mchyba@math.hawaii.edu
[2] University of Hawaii at Manoa, Honolulu, HI. e-mail: jrader@hawaii.edu
[3] University of Hawaii at Manoa, Honolulu, HI. e-mail: andonian@hawaii.edu

Introduction

One of the primary initiatives of the country of Colombia is the constant surveillance of the ever-changing waterways used as shipping lanes. The Magdalena River, the main river of Colombia to which 25% of the Growth Domestic Product (GDP) can be directly associated, is a major shipping lane, as the river penetrates deep into the heart of the country. From southwestern Colombia, it flows approximately 1,000 miles (1,600 km) northward to the Caribbean Sea—past Neiva, Girardot, and the port of Barranquilla (see Fig. 1). Navigable for most of its length, the Magdalena is a major freight artery. For centuries, it has provided a main route to the interior, and its inland waterways transport approximately 3.8 million metric tons of freight and more than 5.5 million passengers annually. Also, said waterways serve as the only means of transportation in 60% of the country due to the lack of navigable roadways.

The Magdalena waterway is one of the most important waterways in the country, accounting for 45 percent of the 2007 cargo movement, *Ministry of Transportation (2008)*. Major products shipped through the Magdalena River are petrochemicals, machinery, cattle, cement, fertilizers, and wood. Due to the river's continuous change, shipping on the river requires trans-shipments and does not operate at full capacity due to lack of investments (totaling 1% of the yearly GDP) in dredging, channel improvements, and protective levies. From Barranquilla to Capulco (about 310 miles), the river is navigable with a depth of only 6 feet allowing night navigation with satellite navigation systems (see Fig. 2). However, due to the impact of many variables, the river must be weekly monitored for depth, currents, and velocity, primarily depth, and especially during the rainy season due to the higher concentration of silt, debris, and/or particulates that can accumulate.

The main way that the monitoring has been done is manually; that is, physical measurements are made by observers on boats. Considering that this is done weekly and over large areas, it is very inefficient and time consuming. We propose a new way of river monitoring by using Autonomous Underwater Vehicles (AUVs) that will, using the most recent map prior to implementing the AUVs, run specific missions in order to obtain the necessary data to create accurate maps for river navigation. Through a variety of missions the AUV will determine actual depths and produce precise maps of said depths, as well as determine river velocities and directions such that precision maps can be produced without requiring physical measurements by observers.

Clearly, this work is still at a very theoretical stage, many additional constraints will have to be taken into account to make it implementable on a real test-bed vehicle. But it provides a first step into that direction.

Mision

The goal is to develop a guidance and navigation algorithm for an AUV to perform high resolution scanning of the constantly changing river bed of the Magdalena River from the river mouth to a distance of 10km upriver, which is considered to be the riskiest section to navigate.

Fig. 1. Satellite view of Magdalena River

We choose to analyze this section since it is considered to be a priority shipping lane and to prevent future shipping failures/groundings. We plan the trajectories of the AUV according to

Fig. 2. Magdalena River

the most recently produced manual bathymetry map. The AUV will be released upstream, dive to a safe depth to avoid surface traffic, will ride the current until it reaches an area of interest, and then will scan, at a depth of around 6-10 meters, considered a navigable depth for all river traffic, in and around these sections that are determined to be deepest from the previous bathymetry map. The missions will include scanning deeper sections of the river to determine exact sizes of these navigable areas and river bathymetry, as well as monitoring river velocity at depths and determining local current directions at cross-sections that are evenly spaced along the river's length. Upon completion of a scanning mission, it will migrate to the next section of interest and will continue so forth until all areas of interest are covered, and/or the battery dies, and/or battery weakens so that the AUV cannot counteract the force of the current, at which point it will migrate downstream until reaching the ocean. Once there, it will surface and send the collected data via satellite as well as a GPS signal so that the AUV can be recovered and it can be recharged and re-released upstream to collect more data. The data will then be used to create a highly, accurate bottom profile and, accordingly, a navigable map that can be used by boat captains. The use of an AUV will significantly minimize the number of persons required previously, as well as the amount of time to collect the bathymetry data. In fact, only one skilled person with access to a ocean- and river-faring boat (with a small crane) and a vehicle (with a lift) is required to perform this task. Also, the data can be collected more regularly than the current weekly collection, thus providing boat captains with daily updates to bathymetry changes.

Although this initially may seem redundant to any captain, if a grounding/sinking occurs, it will be highly apparent to anyone involved in the shipping process (particularly the owners of the boat and cargo) how valuable having accurate, daily-produced bathymetry maps truly is.

Vehicle Design

The chosen design of the vehicle has been determined by several factors. First, the mission itself imposes specific characteristics to the vehicle such as its shape and actuation mode. An equally critical component in vehicle's design is the controllability capabilities that will be available to complete the mission. Those are determined from several criteria as it is explained below. Our approach here differs from our previous work in which the controllability of the vehicle was a consequence of the vehicle's design. Typically, for missions involving river and long-transect ocean surveys, torpedo-shaped AUVs are used, Fig. 3. The dimensions and characteristics of the vehicle are given in Table 1.

Table 1. Significant Vehicle Dynamic Parameters

Total Mass: 195.76 kg	
M_1 (translational added mass) : 31.43 kg	j_1 (rotational added mass): 0.0704 kg·m^2
M_2 (translational added mass): 66 kg	j_2 (rotational added mass: 4.88 kg·m^2
M_3 (translational added mass): 66 kg	j_3 (rotational added mass): 4.88 kg·m^2
Dimensions: {1.5 m, 0.5 m, 0.5 m}	
Center of Buoyancy (C_B): {0,0,0.007}	Center of Gravity (C_G): {0,0,0}
Buoyant Force, B = ρgv: 1920.4 N	Grav. Force, W = mg : 1920.4 N
D_1: 3.9 kg/m	D_4: 0.13 kg·m^2
D_2: 131 kg/m	D_5: 188 kg·m^2
D_3: 131 kg/m	D_6: 94 kg·m^2

Fig. 3. Shape of the vehicle

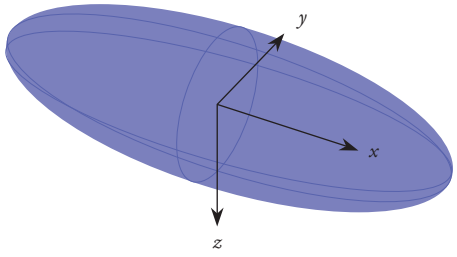

Our vehicle model is based loosely on the Starbug AUV and a REMUS 100 vehicle, which both have similar dimensions. Based on the empirical data of REMUS and the Starbug, we assume the vehicle here has a maximum speed of 1.5 m/s. This is not preposterous by any means, as we've added two additional thrusters, Fig. 4, which would logically have the same capabilities as those on the other two AUVs, to account for the size difference. Added mass terms and drag coefficients are assumed to be similar to those of the REMUS. Such parameters can be found in *Dunababin (2005) and Prestrero (2001)*. Our choice of actuation using thrusters comes from the fact that the AUV will be functioning in a river environment with currents. Gliders are extremely popular and efficient in open ocean, see *Slocum, Remus, and Fleet*, however they do not have the capability to respond quickly to abrupt changes in the environment and, therefore, are not suitable for river surveys. Our goal here is to produce a thruster configuration using a minimal number of thrusters but allowing maximum flexibility and controllability. To this end, we refer to previous work on kinematic controllability *Smith (2009a)*. In *Smith (2009a)*, it has been shown that any combination of one translation and two rotational degrees of freedom provides a system that is kinematically controllable. More precisely, an underwater vehicle with direct control in either one of the translation motion (surge, sway, heave) as well as two rotational motions (roll, pitch, sway) can reach any configuration by the use of integral curves of the decoupling vector fields (see section on Control Design) corresponding to this actuation configuration scenario. Our choices of the directly controllable degrees of freedom are surge, yaw, and pitch. This is motivated by the river environment in which the vehicle interacts. From our thruster configuration, we note that our vehicle begins (and will remain) under-actuated. Thus, the only permissible degrees of freedom available to us correspond to surge, pitch, and yaw motions. Moreover, the four thrusters contributing to surge and yaw give us a bit of a leeway in the event of thruster failure. If a thruster on either side were lost, we would retain controllability over surge and yaw, albeit maximum thruster power is no longer available. Given our thruster configuration, it is necessary to have a linear transformation which takes the geometric controls in the available three degrees of freedom from the body-frame and yields the needed controls for each thruster to accomplish said motion. This corresponds to the matrix given below,

$$T = \begin{pmatrix} -0.24885 & 0 & 0.48733 \\ 0.24885 & 0 & -0.48733 \\ -0.24885 & 0 & -0.48733 \\ 0.24885 & 0 & 0.48733 \\ 0 & 0.65972 & 0 \end{pmatrix} \quad (1)$$

Moreover, we will set the maximum force output of any thruster to be 2.25 Newtons (N). Thus, the maximum force of the four thrusters contributing to surge and yaw is 9 N. This means the front, vertical thruster has a maximum torque of 6.75 Newton-meters (Nm).

Fig. 4. Thruster's Configuration

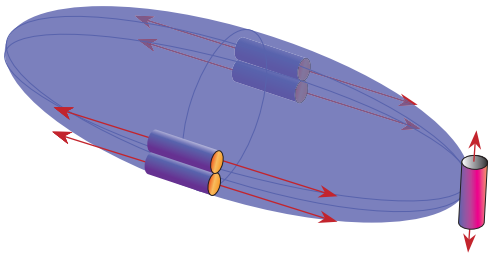

Control Design

The calculations of the dynamic controls to achieve the AUV mission are done in several steps. First, based on our choice of the thruster's configuration, we determine a path in the configuration space

for our vehicle to survey pre-determined areas of the river. This is done through a concatenation of kinematic motions. Second, using an inverse kinematic procedure, we compute the corresponding controls for the dynamic system. The inverse kinematic procedure does not allow for the incorporation of restoring forces and moments nor for the current of the water. A third step is necessary to compensate for the fact that our vehicle is not neutrally buoyant and that the center of gravity and buoyancy do not coincide. And finally the current of the river is taken into account in the calculations of the dynamic controls. Once all the steps have been completed, the vehicle will follow the prescribed path in the configuration space using the calculated thrust.

Kinematic motions

We present a typical motion in the configuration space (position + orientation) to realize the AUV's mission. As mentioned before, the degrees of freedom that are directly controlled are surge (a natural choice in the environment as it is aligned with the river current) coupled with yaw and pitch. This pair of angular degrees of freedom is arbitrary in choice (we could have opted for a combination of yaw/roll or roll/pitch to achieve motion in all six degrees), but this choice is more relevant in reference to the kinematic paths designed for the AUV. We chose the yaw and pitch angles specifically so that the motions in the induced directions (sway and heave) could be facilitated by the force of the current to conserve the AUV's energy, which is important in considering how the AUV would survey the specific region of choice, in this case an arbitrary rectangular region. To be able to apply our theory to compute the dynamic controls, we must insure that the kinematic paths can be obtained as integral curves of decoupling vector fields for the given thruster's configuration. We refer the reader to *Smith (2009a)* for more information about the theoretical calculations of our strategy. In short, the idea is that the decoupling vector fields are of kinematic reduction of rank one, and their integral curves represent motion in the configuration space that are called kinematic motions. The important feature of kinematic motions is that they are feasible by the actual vehicle, or in other words it means that, through an inverse kinematic procedure, we can determine the power output that the thrusters must provide to follow the motion exactly. We chose paths such that the long axis of the vehicle is aligned parallel to the river current (when in the standard orientation) as often as possible as to minimize drag forces caused by the current (to be as hydrodynamic as possible), and when not in standard orientation, the vehicle utilizes the current. Once the vehicle reached an area of interest, it performs transects perpendicular to the river current, as opposed to parallel transects. The reason for this choice comes from the fact that the total amount of energy required for parallel transects would be much greater than the total energy required for perpendicular transects. Indeed, during a pair of parallel transects the vehicle initially uses zero energy since it is riding the current downstream, but after moving to the next parallel transect, which is now oriented upstream, the vehicle has to fight the current to reach the original location and requires large amounts of energy, not to mention the energy needed by the AUV to move from one transect to the next. However, in the perpendicular transects, the vehicle uses a constant amount of energy only to balance the drag forces and maintain its orientation, and moving to the next perpendicular transect requires zero energy as the vehicle rides the current downstream to it. Hence it is more efficient as it utilizes more of the available energy from the environment.

Dynamic controls

We refer the reader to *Bullo-Lewis (2004)*, and *Smith (2009b)*, for a complete treatment on the inverse procedure to obtain the dynamic controls. It is out of the scope of this paper to repeat those derivations here. It has to be noted, however, that the inverse procedure provide the dynamic controls without taking into account the restoring and potential forces as well as the river current. How to compensate for the restoring and potential forces can be found for instance in *Andonian et al. (2010)*. We are explicit in this paper how to adjust the controls to take into account the river's current, see section on Simulations.

Simulations

In this section, we bring life to the theory by considering a simulation using the vehicle and mission plan described previously. The environment we are simulating, the Magdalena River in Fig. 5, is particularly interesting due to the fact we must now account for the river's flow. We assume the current of the river has a constant velocity of 2 m/s throughout depths of 0-5 meters, a constant velocity of 1.5 m/s throughout depths of 5-7 meters, and a constant velocity of 1 m/s throughout depths of 7-12 meters. These values are based on data from the Laboratorio Las Flores from Cormagdalena-Uninorte in Barrancabermeja, Colombia. As usual, the positive vertical axis of the inertial frame is in the direction of gravity.

Fig. 5. Simulated Magdelena Environment. Scale 1:16

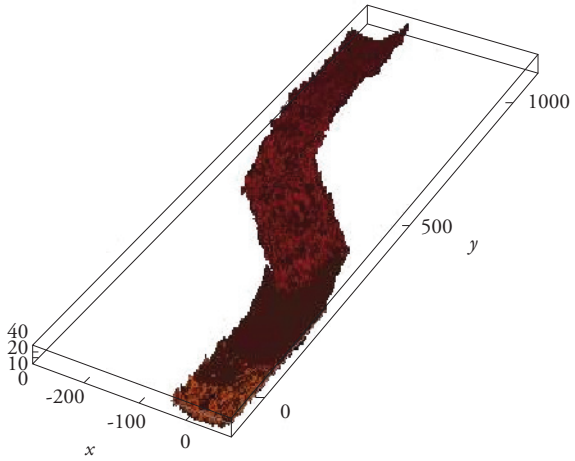

In Table 2, we give a full reference for each of the eight phases of the mission. The configuration and time for each phase can be found in Table 3 of the Appendix.

Let us now begin the simulation of the mission. The vehicle will be initially deployed upstream and travel downstream until it reaches a desirable section. We assume the AUV is oriented to be "facing" downstream and assume it is five meters below the surface. The symbol, η, will represent a vector whose first three components refer to the vehicle's position and the last three components to orientation, in terms of Euler angles, in the inertial frame. Our initial configuration will be where the vehicle begins its mission. As such, the origin of the inertial frame will be taken at the surface of the water before the exploration mission begins. Thus, the initial configuration is,

Table 2. Description of AUV River Survey Mission

Phase No.	Description of Phase
1	Achieve and maintain desired orientation
2	Dive
3	Reorient parallel to river current
4	Rotate 45 degrees left
5	Surge
6	Rotate 90 degrees right
7	Surge
8	Rotate 90 degrees left and repeat

$$\eta_0 = (0,0,5,0,0,0) \tag{2}$$

Note, the velocity of the river's current exceeds the vehicle's maximum speed; thus, if we do not compensate for this speed difference, we will obviously drift past the target. More on this point will be discussed later. For the first phase, the vehicle pitches 45 degrees towards the riverbed and maintains this angle. Since $C_G \neq C_B$, there are righting moments we must consider. In general for our system, they are given by,

$$P(\gamma)(t)) = \begin{pmatrix} 0 \\ 0 \\ 0 \\ 0 \\ z_B B\sin\theta \\ 0 \end{pmatrix} \tag{3}$$

where B is the buoyancy force and z_B is the z-coordinate for the location of the center of buoyancy of the vehicle. For the second phase, the vehicle descends at this 45 degree angle for 25 seconds until it reaches the 10.89 meters in depth. Fig. 7 gives the six plots for the configurations throughout this phase, beginning at η_1 and ending at η_2.

Fig. 6. Position Plots of the AUV's Path for Phase 2 of the Mission

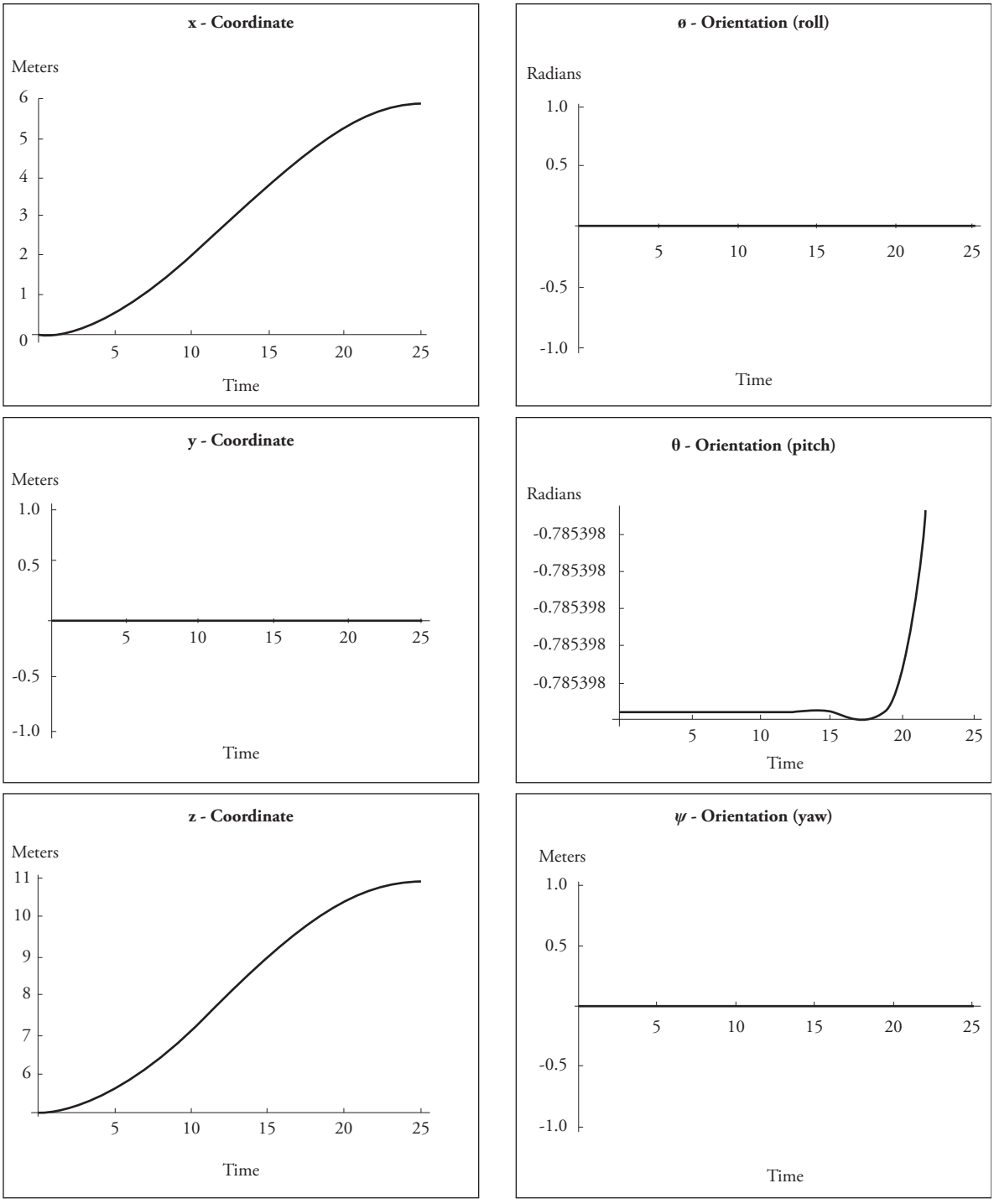

At this point, we are in an area of the river where the vehicle's maximum speed exceeds the river's current. The third phase of the mission involves the vehicle reorienting itself to become parallel with the river's surface again. During the fourth phase, the vehicle must counteract the river's current. The vehicle then proceeds to survey the riverbed as described in phases 5 – 9 in Table 2.

The final phase has the vehicle reorienting itself parallel to the current yet again. Fig. 8 shows plots of the necessary forces for each of the thrusters

Fig. 7. Necessary Thruster Forces for a Left Turn

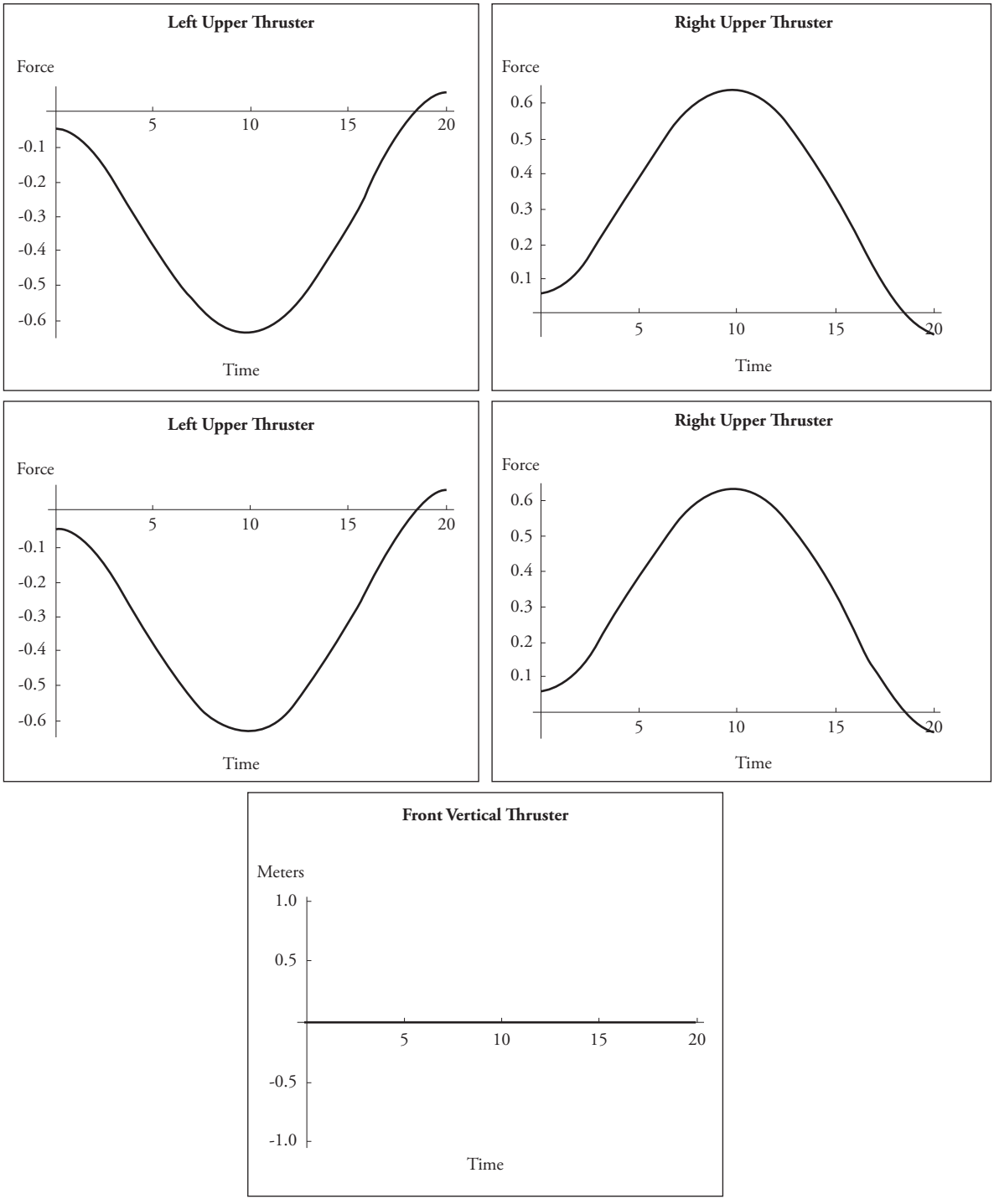

in order to turn 45 degrees to the left. Due do the redundancy in our control strategy, note the negative values for each of these thruster force plots corresponds to the necessary forces to turn the vehicle 45 degrees to the right. The vehicle must then repeat phases 4-8 until enough data is collected to complete the mission objective. We now move on to the second half of the simulation discussion and adjust our controls to account for the river current.

Let us define our controls to be $\sigma_{i,j}$ where i refer to the mission phase and j is the jth component of the configuration. In addition, we assume these $\sigma_{i,j}$'s already have the necessary restoring forces included. Similarly, we will define $\tau_{i,j}$ to be the adjusted controls that compensate for the river current. These controls correspond to the body-fixed frame, geometric controls. Recall that the maximum forward thrust of the vehicle is 9 N and the maximum torque is 6.75 Nm.

Now turning our focus to phase one of the mission plan, we must determine the required control's adjustment in order to maintain our pitch of 45 degrees pointing down towards the river bed given the river's current. Theoretically, if the vehicle is in a horizontal orientation, and was to maintain a velocity of 2 m/s, it would need to exert 15.74 Newtons of force; this force would keep the vehicle stationary in the river and so we will assume 15.74 N is the amount of force exerted on the vehicle by the river's current at 2 m/s. With the vehicle pitched as it is in phase one, the current will induce a moment on the vehicle. Assuming the vehicle is a point mass at the center of gravity, we utilize classical physics to calculate the torque the vehicle would need to exert to maintain its pitch.

Thus, the "lever arm" is the distance from the center of gravity to the vertically mounted thruster, which is 0.75 meters. Fig. 8 shows a side profile of the vehicle and the significant parameters. Since we are only concerned with our pitch angle, all other controls are zero. Using Fig. 8 as a basis, we find the torque acting on the portion of the vehicle above the dotted line is given by

$$\omega_{top} = \frac{\sqrt{2}}{2}\begin{pmatrix}0.75\\0\\0.75\end{pmatrix} \times \begin{pmatrix}15.74\\0\\0\end{pmatrix} = \begin{pmatrix}0\\8.35\\0\end{pmatrix} \cdot \quad (4)$$

Thus, there is a torque of 8.35 Nm that must be considered in the controls. Let us remark again that the vehicle is assumed to be experiencing a constant force above the dotted line and below the dotted line. This allows us to simply sum all the torques to find what kind of moment we must counteract. This gives us a new control

$$\tau_{1,5}(t) = \sigma_{1,5}(t) + 8.35 \quad (5)$$

where the additional torque is added to the original controls. We added this torque due to the fact that the current at 2 m/s is righting our pitching motion. However, the vehicle is also experiencing a force below the dotted line. This torque turns out to be

$$\omega_{bottom} = \frac{\sqrt{2}}{2}\begin{pmatrix}-0.75\\0\\-0.75\end{pmatrix} \times \begin{pmatrix}8.92\\0\\0\end{pmatrix} = \begin{pmatrix}0\\-4.73\\0\end{pmatrix} \cdot \quad (6)$$

which ultimately (by summing the torques) gives us the control we need to maintain the pitch,

$$\tau_{1,5}(t) = \sigma_{1,5}(t) + 3.62 \quad (7)$$

Note, we are within our bounds.

Fig. 8. Side View of AUV pitched 45 Degrees towards the River Bed where χ=0.75*sin(45°)* and β=0.75*cos(45°)*

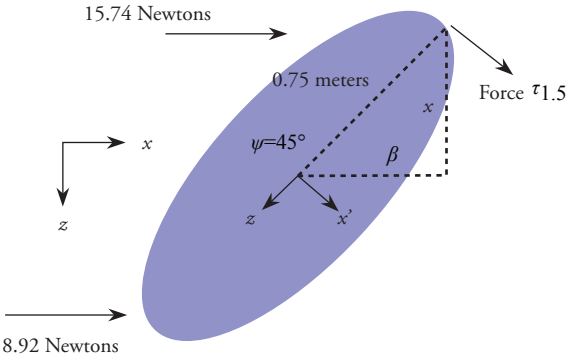

For phase 2, the situation gets more complicated. As the vehicle descends into the river, the velocity of the current acting on the vehicle changes. For these controls, we will assume the vehicle must counteract the most powerful forces to not drift backwards. Thus, from Fig. 7 we can assert the vehicle does not completely pass through the 2 m/s current until t = *15.7s* and does not pass through the 1.5 m/s current until t = *22s*. The force needed to counteract the 2 m/s current during the dive is 22.19N (note that this force is higher than 15.74N due to the fact that the vehicle is maintaining a

pitch), and to counteract the 1.5 m/s current is 12.58N. However, these are outside the maximum thruster output of the vehicle, so we will drift downstream. Then, at time $t = 22s$, the vehicle completely passes into the region of the river where the current velocity is 1 m/s. To remain stationary at this pitched angle, the vehicle must apply 5.7N of forward thrust. However, once the vehicle completely passes into 1 m/s flow range, there are no longer any moments to account for. Our controls now become

$$\tau_2(t) = \begin{cases} \tau_{2,1}(t) = \begin{cases} 9 & t\in[10,15.7] \\ -0.25(t-35)+5.75 & t\in[22,35] \\ 0 & \end{cases} \\ 0 \\ 0 \\ \tau_{2,5}(t) = \begin{cases} \sigma_{2,5}(t) - 1.465(t-10)+3.62 & t\in[10,15.7] \\ 0.41(t-10)-4.73 & t\in[15.7,22] \\ 0 & t\in[22,35] \end{cases} \\ 0 \end{cases} \quad (8)$$

to complete phase two. Now, we look to discover the necessary controls to complete phase 3. We will assume it takes ten seconds still to reorient the vehicle. However, we wish to remain stationary for an additional 30 seconds. Again, we need not worry about the force of the current causing a moment on the AUV, as the sum of the torques is zero. As such, the only control we are searching for corresponds to surge; the sway control on the other hand remains the same as before without the river current. The initial body-frame forward thrust will still be 5.7 N to not surge, dive, or drift and will end with a thrust force of 4.04 N, which is the force we need to remain stationary with the vehicle parallel to the current flow. Thus, the new controls running from $t = 35s$ to $t = 45\ s$ are

$$\tau_3(t) = \begin{cases} \tau_{3,1}(t) = -5.7 + 0.166(t-35) \\ 0 \\ 0 \\ 0 \\ \sigma_{3,5}(t) \\ 0 \end{cases} \quad t\in[35,45]. \quad (9)$$

Finally, we compute the necessary controls for phases 4, 5, and 6. Due to the redundancy of this control strategy, we need not compute the remaining controls, as they will be the same but simply allocated differently to the thrusters. For phase four, we must perform a yaw maneuver to turn left. Since we begin to experience a moment as soon as we begin the turn left, we will assume we must compensate for this torque the entire time. This torque is the same as before 2.14 Nm, but in a different plane. The same can be said about the compensating thruster force to keep the vehicle from drifting in the y-plane; this must be 4.04 N initially and 5.7 N when the vehicle has rotated 45 degrees to the left. Assuming the time it takes the vehicle to rotate remains ten seconds, beginning at $t = 45s$ and ending at $t = 55s$, our controls become

$$\tau_4(t) = \begin{cases} \tau_{4,1}(t) = -4.04 - 0.166(t-45) \\ 0 \\ 0 \\ 0 \\ 0 \\ \sigma_{4,6}(t) \end{cases} \quad t\in[45,55]. \quad (10)$$

Note that there are no moments we must compensate for. This is because the sum of the torques acting on the vehicle at any angle for parallel with the river's flow will again be zero. For phase five, we adjust our controls only slightly to compensate for the current,

$$\tau_{5,1}(t) = \begin{cases} -5.7 & t\in[55,67.7] \\ \sigma_{5,1}(t) - 11.4 & t\in[67.7,95.1] \\ -5.7 & t\in[95.1,115] \end{cases} \quad (11)$$

And finally, we wish to execute phase six; the necessary controls are

$$\tau_6(t) = \begin{cases} \tau_{6,1}(t) = -(0.0166t^2 - 5.416t + 402.855) \\ 0 \\ 0 \\ 0 \\ 0 \\ \sigma_{6,6}(t) \end{cases} \quad t\in[115,135]. \quad (12)$$

Figures 9a and 9b represent simulations in the river environment of Phases 2 and 4, respectively, of the mission. In the figures, the dashed orange vectors correspond to the river current velocity at 2.0 m/s, the dotted blue vectors correspond to the river current velocity at 1.5 m/s, and the solid white vectors correspond to the river current velocity at 1.0 m/s. Also, the vehicle is magnified by a factor of 8 for visualization purposes only.

Fig. 9a. Phase 2 Trajectory of Mission

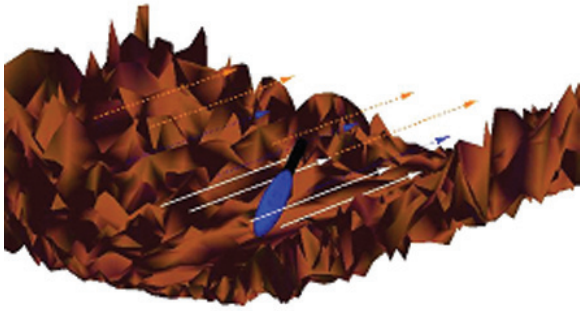

Fig. 9b. Phase 4 Trajectory of Mission

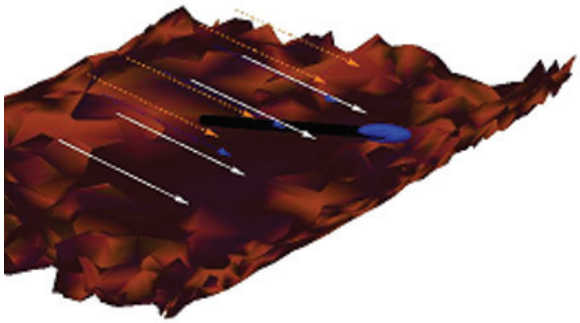

References

ANDONIAN, M., CAZZARO, L., INVERNIZZI, L, and CHYBA, M. *Geometric Control for Autonomous Underwater Vehicles: Overcoming a Thruster Failure.* IEEE Conference on Decisions and Control. Atlanta, GA. 2010.

BULLO, F. and LEWIS, A. *Geometric Control of Mechanical Systems,* Texts in Applied Mathematics, Springer, ISBN 0-387-22195-6, 2004.

DUNBABIN, M., ROBERTS, J., USHER, K., WINSTANLEY, G., and CORKE, P. *A Hybrid AUV Design for Shallow Water Reef Navigation*. IEEE. Proceedings of the 2005 IEEE International Conference on Robotics and Automation. Barcelona, Spain. 2005.

FLEET. *http://marine.reutgers.edu/cool/auvs/*

MINISTRY OF TRANSPORTATION, Oficina Asesora de Planeacion, Grupo de Planificacion Sectorial, *Diagnóstico del Sector Transporte,* 2008. http://www.mintransporte.gov.co/Servicios/Estadisticas/home.htm

PRESTERO, T. *Verification of a Six-Degree of Freedom Simulation Model for the REMUS Autonomous Underwater Vehicle.* Master's thesis. Massachusetts Institute of Technology and Woods Hole Oceanographic Institution, Joint Program in Applied Ocean Science and Engineering. 2001.

REMUS. *http://www.hydroidinc.com/*

SLOCUM. *http://www.webbresearch.com/slocumglider.aspx*

SMITH, R. and CHYBA, M. *Trajectory Design for Autonomous Underwater Vehicle for Basin Exploration*. 8th International Conference on Computer Applications and Information Technology in the Maritime Industries (COMPIT), Budapest 2009

SMITH, R., CHYBA, M., WILKENS, G., and CATONE, C. *A Geometrical Approach to the Motion Planning Problem for a Submerged Rigid Body*. International Journal of Control, Vol. 82/9, pp. 1641 -1656, 2009.

Appendix

Table 3. Reference Velocities and Configurations for AUV River Survey (No Current)

Phase No.	Initial Time (sec)	Final time (sec)	Reference Velocity	Initial Configuration	July 8
1	**0**	$t_1 = 10$	$\begin{pmatrix} 0 \\ 0 \\ 0 \\ 0 \\ -\frac{\pi}{40} \\ 0 \end{pmatrix}$	η_0	$\eta_1 = \begin{pmatrix} 0 \\ 0 \\ 5 \\ 0 \\ -\frac{\pi}{4} \\ 0 \end{pmatrix}$
2	$\mathbf{t_1}$	$t_2 = 35$	$\begin{pmatrix} \frac{1}{3} \\ 0 \\ 0 \\ 0 \\ 0 \end{pmatrix}$	η_1	$\eta_2 = \begin{pmatrix} 0 \\ 5.89 \\ 10.89 \\ 0 \\ -\frac{\pi}{4} \\ 0 \end{pmatrix}$
3	$\mathbf{t_2}$	$t_3 = 45$	$\begin{pmatrix} 0 \\ 0 \\ 0 \\ 0 \\ \frac{\pi}{40} \\ 0 \end{pmatrix}$	η_2	$\eta_3 = \begin{pmatrix} 0 \\ 5.89 \\ 10.89 \\ 0 \\ 0 \\ 0 \end{pmatrix}$
4	$\mathbf{t_3}$	$t_4 = 55$	$\begin{pmatrix} 0 \\ 0 \\ 0 \\ 0 \\ 0 \\ \frac{\pi}{40} \end{pmatrix}$	η_3	$\eta_4 = \begin{pmatrix} 0 \\ 5.89 \\ 10.89 \\ 0 \\ 0 \\ \frac{\pi}{4} \end{pmatrix}$
5	$\mathbf{t_4}$	$t_5 = 115$	$\begin{pmatrix} 1 \\ 0 \\ 0 \\ 0 \\ 0 \\ 0 \end{pmatrix}$	η_4	$\eta_5 = \begin{pmatrix} 42.43 \\ 48.31 \\ 10.89 \\ 0 \\ 0 \\ \frac{\pi}{4} \end{pmatrix}$
6	$\mathbf{t_5}$	$t_6 = 135$	$\begin{pmatrix} 0 \\ 0 \\ 0 \\ 0 \\ 0 \\ -\frac{\pi}{40} \end{pmatrix}$	η_5	$\eta_6 = \begin{pmatrix} 42.43 \\ 48.31 \\ 10.89 \\ 0 \\ 0 \\ -\frac{\pi}{4} \end{pmatrix}$
7	$\mathbf{t_6}$	$t_7 = 195$	$\begin{pmatrix} 1 \\ 0 \\ 0 \\ 0 \\ 0 \\ 0 \end{pmatrix}$	η_6	$\eta_7 = \begin{pmatrix} 84.86 \\ 5.89 \\ 10.89 \\ 0 \\ 0 \\ -\frac{\pi}{4} \end{pmatrix}$
8	$\mathbf{t_7}$	$t_8 = 215$	$\begin{pmatrix} 0 \\ 0 \\ 0 \\ 0 \\ 0 \\ \frac{\pi}{40} \end{pmatrix}$	η_7	$\eta_8 = \begin{pmatrix} 84.86 \\ 5.89 \\ 10.89 \\ 0 \\ 0 \\ \frac{\pi}{4} \end{pmatrix}$

Metamodeling Techniques for Multidimensional Ship Design Problems

Técnicas para el desarrollo de metamodelos aplicadas a problemas multidimensionales en el diseño de barcos

Peter B. Backlund[1]
David Shahan[2]
Carolyn C. Seepersad[3]

Abstract

Metamodels, also known as surrogate models, can be used in place of computationally expensive simulation models to increase computational efficiency for the purposes of design optimization or design space exploration. Metamodel-based design optimization is especially advantageous for ship design problems that require either computationally expensive simulations or costly physical experiments. In this paper, three metamodeling methods are evaluated with respect to their capabilities for modeling highly nonlinear, multimodal functions with incrementally increasing numbers of independent variables. Methods analyzed include kriging, radial basis functions (RBF), and support vector regression (SVR). Each metamodeling technique is used to model a set of single-output functions with dimensionality ranging from one to ten independent variables and modality ranging from one to twenty local maxima. The number of points used to train the models is increased until a predetermined error threshold is met. Results show that each of the three methods has its own distinct advantages.

Key words: Metamodeling, kriging, radial basis functions, support vector regression, metamodel-based design optimization.

Resumen

Los metamodelos, también conocimos como modelos substitutos, pueden ser utilizados en lugar de modelos cuyas simulaciones tienen un costo computacional muy alto, incrementado con esto la eficiencia en procesos de optimización de diseños o en el diseño de exploraciones espaciales. La optimización de diseños basados en metamodelos es especialmente ventajosa en problemas de diseño relacionado con vehículos marinos en los cuales se requieran simulaciones con un alto costo computacional o bien de experimentos con una alta inversión en equipos. En este artículo se evalúan tres métodos para el desarrollo de metamodelos. La evaluación de estos métodos es desarrollada teniendo en cuenta la capacidad de cada uno de ellos para modelar funciones multimodales no lineales con un número creciente de variables independientes. Dentro de los métodos analizados se encuentran el método de kriging, el método de funciones de base radiales, y el método de regresión con vector de apoyo. Cada una de las anteriores técnicas para la generación de metamodelos es utilizada para modelar un grupo de funciones de una salida con dimensiones variando desde uno hasta diez variables independientes y una modalidad variando entre uno y veinte máximos locales. El número de puntos utilizados para entrenar los modelos es incrementado hasta que el error alcanza una tolerancia predeterminada. Los resultados obtenidos muestran que cada uno de los tres modelos tiene sus propias ventajas distintivas.

Palabras claves: Desarrollo de metamodelos, kriging, funciones de base radiales, regresión con vector de apoyo, optimización de diseños basada en metamodelos.

Date received: May 19th, 2010. - *Fecha de recepción: 19 de Mayo de 2010.*
Date Accepted: July 6, 2010. - *Fecha de aceptación: 6 de Julio de 2010.*

[1] Applied Research Laboratories. The University of Texas. Austin, TX. USA. e-mail: pbacklund@mail.utexas.edu
[2] The University of Texas. Austin, TX. USA. e-mail: david.shahan@mail.utexas.edu
[3] The University of Texas. Austin, TX. USA. e-mail: ccseepersad@mail.utexas.edu

Introduction

Computer models of naval systems and other physical systems are often complex and computationally expensive, requiring minutes or hours to complete a single simulation run. While the accuracy and detail offered by a well constructed computer model are indispensable, the computational expenseof many models makes it challenging to use them for design applications. For example, objective functions for ship hull design problems commonly include payload, ship speed, motions, and calm-water drag *(Percival et al., 2001)*. In many cases, computational fluid dynamics (CFD) models are used as tools to analyze performance characteristics of candidate designs *(Periet al., 2001)*. Unfortunately, CFD simulations tend to be computationally expensive and time consuming to execute and therefore limit a designer's ability to explore a broad range of configurations or interface the simulation with design optimization algorithms that require numerous, iterative solutions.

To remedy this situation, metamodel scan bedeveloped as surrogates of the computer model to provide reasonable approximations in a fraction of the time. Metamodels are developed using a set of training points from a base model. Once built, the metamodel is used in place of the base model to predict model responses quickly and repeatedly. For example, a metamodel built using a set of training points from a CFD model could enable ship designers to find satisfactory hull forms more rapidly than by using the base model alone. Other possible applications of metamodels to ship design problems include optimization of marine energy systems *(Dimopouloset al., 2008)*, propeller design *(Watanabe et al., 2003)*, and marine vehicle maneuvering problems *(Racine and Paterson, 2005)*. In this paper, the focus will be on designing thermal systems for ship applications.

The best metamodeling method for a particular application depends on the needs of the project and the nature of the base model that is to be approximated. Five common criteria for evaluating metamodels include:

- ***Accuracy:*** Capability of predicting new points that closely match those generated by the base model.
- ***Training Speed:*** Time to build the metamodel with training data from the base model.
- ***Prediction Speed:*** Time to predict new points using the constructed metamodel.
- ***Scalability:*** Capability of accommodating additional independent variables.
- ***Multimodality:*** Capability of modeling highly nonlinear functions with multiple regions of local optimality (modes).

No single metamodeling method has emerged as universally dominant. Rather, individual techniques have strengths and weaknesses. Selection of the method is dependent on several factors such as the nature of the response function, and the availability of training data. Methods that most frequently appear in the literature are response surface methodology (RSM) *(Box and Wilson, 1951)*, multivariate adaptive regression splines (MARS) *(Friedmanl, 1991)*, support vector regression (SVR) *(Vapniket al., 1997)*, kriging *(Sacks et al., 1989)*, radial basis functions (RBF) *(Hardy, 1971)*, and neural networks *(Haykin, 1999)*.

In this research study, kriging, radial basis functions (RBF), and support vector regression (SVR) are used to model a set of functions with varying degrees of scale and multimodality. In Section 2, related research is reviewed, and the rationale for selecting kriging, RBF, and SVR for this study is discussed. In Section 3, the test functions and experimental design for this study are explained. Results are presented in Section 4, and closing remarks are made in Section 5.

Review of Metamodeling Methods

Detailed Descriptions of Methods Under Consideration

Polynomial Regression

Polynomial regression (PR) *(Box and Wilson, 1951)*

models the response as an explicit function of the independent variables and their interactions. The second order version of this method is given in (1):

$$\hat{y}(\mathrm{x}) = \beta_0 + \sum_{i=1}^{m} \beta_i x_i + \sum_{i=1}^{m} \beta_{ii} x_i^2 \quad \sum_{i=1}^{m} \sum_{i=2,i<j}^{m} \beta_{ij} x_i x_j \tag{1}$$

where the x_i are the independent variables and the β_i are coefficients that are obtained with least squares regression.

Polynomial regression is a global approximation method that presumes a specific form of the response (linear, quadratic, etc.). Therefore, polynomial regression models are best when the base model is known to have the same behavior as the metamodel. Studies have shown that polynomial regression models perform comparable to kriging models, provided that the base function resembles a linear or quadratic function *(Giunta and Watson, 1998; Simpson et al., 1998).*

Kriging

Kriging *(Sacks et al., 1989)* consists of a combination of a known global function plus departures from the base model, as shown in (2):

$$\hat{y}(\mathbf{x}) = \sum_{j=1}^{k} \beta_i f_i(\mathbf{x}) + Z(\mathbf{x}) \tag{2}$$

where β_i are unknown coefficients and the $f_i(\mathbf{x})$'s are pre-specified functions (usually polynomials). $Z(\mathbf{x})$ provides departures from the underlying function so as to interpolate the training points and is the realization of a stochastic process with a mean of zero, variance of σ^2, and nonzero covariance of the form

$$\mathrm{cov}[Z(x_i), Z(x_j)] = \sigma^2 R(x_i, x_j) \tag{3}$$

where R is the correlation function which is specified by the user. In this study, a constant term is used for $f(\mathbf{x})$ and a Gaussian curve of the form in (4) is used for the correlation function:

$$R(x_i, x_j) = \exp\left[-\theta_i (x_i - x_j)^2\right] \tag{4}$$

where the θ_i terms are unknown correlation parameters that are determined as part of the model fitting process. The automatic determination of the θ_i terms makes kriging a particularly easy method to use. Also, contrary to polynomial regression, a krigingmetamodelof this form will always pass through all of the training points and therefore should only be used with deterministic data sets.

Kim et al. *(Kim et al., 2009)* show that kriging is a superior method when applied to nonlinear, multimodal problems. In particular, kriging outperforms its competitors when the number of independent variables is large. However, it is well documented that kriging is the slowest with regard to build time and prediction time compared with other methods *(Jin et al., 2001; Ely and Seepersad, 2009).*

Radial Basis Functions

Radial basis functions *(Hardy, 1971)* use a linear combination of weights and basis functions whose values depend only on their distance from a given center, $\mathbf{x}_i$. Typically, a radial basis function metamodel takes the form (5):

$$\hat{y}(\mathrm{x}) = \sum_{j=1}^{k} w_i \phi_i(\mathrm{x}, \mathrm{x}_i) \tag{5}$$

where the w_i is the weight of the i_{th} basis function, ϕ_i. In this study, a Gaussian basis function of the form in (6) is used to develop the metamodels for testing:

$$\phi(\mathrm{x}, x_i) = \exp\left[-k \left\| \mathrm{x} - \mathrm{x}_i \right\|^2\right] \tag{6}$$

where k is a user specified tuning parameter.

Radial basis function metamodels are shown to besuperior in terms of average accuracy and ability to accommodate a large variety of problem types *(Jin et al., 1999).* However, Kim et al. *(Kim et al., 2009)* show that prediction error increases significantly for RBF as the number of dimensions increases. This pattern suggests caution must be used when applying RBF to high dimensional problems to ensure that proper tuning parameters are used. RBF is also shown to be moderately more computationally expensive than other methods such as polynomial regression *(Fang et al., 2005).*

Support Vector Regression

In support vector regression *(Vapniket al., 1997)*, the metamodel takes the form given in (7):

$$\hat{y}(\mathrm{x}) = \sum_{i=1}^{l} (a_i - a_i^*)\, k\,(\mathrm{x}_i, \mathrm{x}) + b \tag{7}$$

where the a terms are Lagrange multipliers, $k(\mathbf{x}_i,\mathbf{x})$ is a user specified kernel function, and b is the intercept. The a terms are obtained by solving the following dual form optimization problem:

$$\text{Maximize} \begin{cases} -\frac{1}{2} = \sum_{i,j=1}^{l} (a_i - a_i^*)(a_j - a_j^*)\, k\,(\mathrm{x}_i, \mathrm{x}_j) \\ -\varepsilon = \sum_{i=1}^{l} (a_i - a_i^*) + \sum_{i=1}^{l} y_i (a_i - a_i^*) \end{cases} \tag{8}$$

$$\text{Subject to} \begin{cases} \sum_{i=1}^{l} (a_i - a_i^*) = 0 \\ a_i - a_i^* \in [0, C] \end{cases} \tag{9}$$

In (8) and (9), l is the number of training points, ε is a user defined error tolerance, and C is a cost parameter that determines the trade-off between the flatness of the $\hat{y}$ and the tolerance to deviations larger than ε. In this study, a Gaussian kernel function of the form in (10) is used to construct the metamodels for testing:

$$k\,(\mathbf{x}, x_i) = \exp[\, -g(\mathbf{x} - \mathrm{x}_i)^2] \tag{10}$$

where g is a user specified tuning parameter.

Clarke et al. *(Clarke et al., 2005)* indicate that SVR has the lowest level of average error when applied to a set of 26 linear and non-linear problems when compared to polynomial regression, kriging, RBF, and MARS. SVR has also been shown to be the fastest method in terms of both build time and prediction time *(Ely and Seepersad, 2009)*. An unfortunate drawback of SVR is that accurate models depend heavily on the careful selection of the user defined tuning parameters *(Lee and Choi, 2008)*.

Multivariate Adaptive Regression Splines

Multivariate adaptive regression splines (MARS) *(Friedmanl, 1991)* involves partitioning the response into separate regions, each represented by their own basis function. In general, the response has the form given in (11):

$$\hat{y}(\mathbf{x}) = \sum_{m=1}^{M} a_m B_m(\mathbf{x}) \tag{11}$$

where a_m are constant coefficients and $B_m(\mathbf{x})$ are basis functions of the form

$$B_m(\mathrm{x}) = \prod_{k=1}^{K_m} [s_{k,m}(x_{v(k,m)} - t_{k,m})\,]_+^q \tag{12}$$

In the Equation (12), K_m is the number of splits in the M^{th} basis function, $s_{k,m}$ take values ±1, $x_{v(k,m)}$ are the test point variables, and $t_{k,m}$ represent the knot locations of each of the basis functions. The subscript "+" indicates that the term in brackets is zero if the argument is negative. MARS adaptively partitions the design space into sub-regions that have their own regression equations, which enables it to model nonlinear and multimodal responses in high dimensional space.

MARS is shown to predict as well as other methods, but only when a large set of training data is available *(Wang et al., 1999, Jin et al., 2001)*. Using MARS is particularly challenging compared with other methods due to the number of user defined parameters that must be selected. When a large number of basis functions is required to build an accurate model (i.e. nonlinear, multimodal), the build time for MARS can be prohibitively large.

Methods Selected for this Study

Based on the literature reviewed in the previous section, several conclusions can be made about the various metamodeling methods. In general, polynomial regression models can be built and executedvery quickly, even in high dimensions. However, polynomial response surfaces are unable to predict highly non-linear and multimodal functions in multiple dimensions. On the other hand, kriging and radial basis functions are both capable of modeling nonlinear and multimodal functions with higher computation time than polynomial regression. Multivariate adaptive regression splines are capable of modeling multimodal functions in high dimensional space,

but often require large training data sets and are computationally expensive to build. Support vector regression, which appears to be the most promising method reviewed here, is shown to be capable of modeling high dimensional multimodal functions accurately with minimal computational expense.

The functions that are modeled in this study range from one to ten dimensions and have modality ranging from one to twenty modes. Polynomial response surfaces are tedious and difficult to construct for multimodal functions due to the exploding number of possible interaction terms that are available for inclusion in the final model. MARS has been shown to be able to model the general behavior of multimodal functions *(Jin et al., 1999)*, but it fails to predict new points accurately at the local maxima and minima. For these reasons, kriging, radial basis functions, and SVR are the primary methods considered in this study.

Test Functions and Experimental Design

To test the ability of polynomial regression, kriging, RBF, and SVR to model functions in high dimensional space, four test functions are used. The first three are generated using a kernel density estimation (KDE) method. The KDE method generates functions in any number of dimensions, containing any number of kernels, where the number of kernels dictates the modality of the resulting surface. The fourth test function is an analytical model of a common engineering system: a two stream counter-flow heat exchanger.

Multidimensional, Multimodal Kernel Based Functions

The need to create test problems of arbitrary dimensionality, D, and arbitrary modality, N, (the number of local maxima or minima) motivates the kernel density estimation (KDE) method. The KDE, also known as a Parzen window *(Parzen, 1992)*, is formulated according to (13) as an average of N kernel functions, K, in product form *(Scott, 1992)*.

$$f(\mathbf{x}) = \frac{1}{N\prod_{i=1}^{D} h_i} \sum_{j=1}^{N} \left[\prod_{i=1}^{D} K\left(\frac{x_i - x_i^j}{h_i} \right) \right] \qquad (13)$$

The shape of the KDE is controlled by the kernel function, the kernel centers, x^j, and the smoothing parameters, h_i. For this research, the triweight kernel function *(Scott, 1992)*, shown in Equation (14), was used for its smoothness and for the fact that it is not a Gaussian function which was used as a basis function for some of the metamodeling techniques studied.

$$K\left(\frac{x_i - x_i^j}{h_i} \right) = \frac{35}{32} \left[1 - \left(\frac{x_i - x_i^j}{h_i} \right)^2 \right]^3 \qquad (14)$$

for $x_i - x_i^j \le h_i$ and K=0 otherwise

Creating a kernel function of arbitrary dimensionality is straightforward. However, controlling the modality is a bigger challenge for which careful consideration of the kernel centers and smoothing parameters is necessary. For the choice of kernel centers, a certain amount of randomness is desired in the resulting function such that it is unique and its structure is unknown in advance of modeling it. However, a certain amount of control over placement of the kernel centers is needed for creating the requested number of distinct peaks and distributing them throughout the design space. This challenge was met by choosing the kernel centers sequentially such that the next center, $\mathbf{x}^{N+1}$, is the minimum of the KDE based on the previous N center points (Equation 15). The first center is chosen from a uniform distribution over the input space.

$$\mathbf{x}^{N+1} = \text{argmin} \left\{ \frac{1}{N\prod_{i=1}^{D} h_i} \sum_{j=1}^{N} \prod_{i=1}^{D} \frac{35}{32} \left[1 - \left(\frac{x_i - x_i^j}{h_i} \right)^2 \right]^3 \right\}$$

$$\text{Subject to: } \mathbf{x}_{min} \le \mathbf{x} \le \mathbf{x}_{max} \qquad (15)$$

This method places the next kernel center at the location of minimum density; hence, the resulting sequence of kernel centers fills the space approximately uniformly. The input space is searched for the minimum using multi-start sequential quadratic programming (fmincon in

Fig. 1a. Two-stream counter-flow heat exchanger. (Mills, 1998)

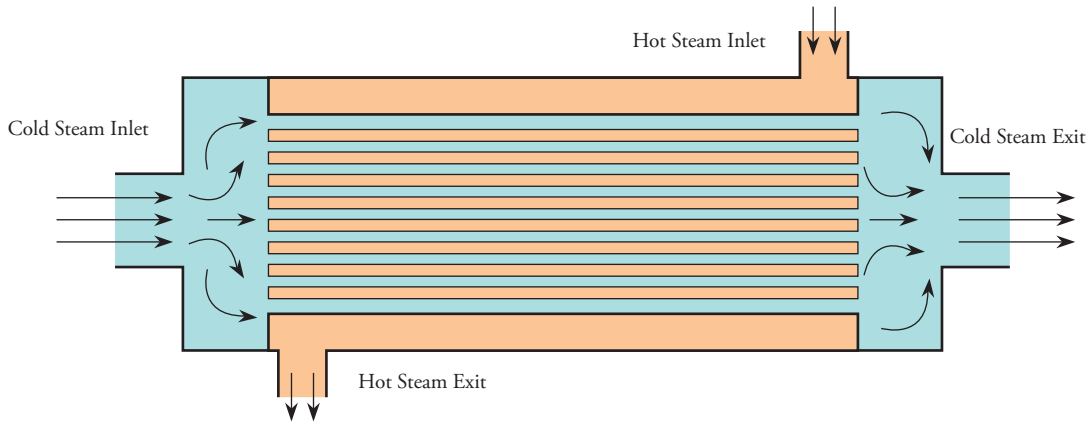

MATLAB®), stopping if more than one second elapses or less than 1% improvement occurs for 5 consecutive sequential quadratic programming iteration.Although this procedure is not guaranteed to find the global minimum, finding the global minimum is not imperative; we only need to find a point in a low density region.

As for the choice of smoothing parameter, setting it too small will result in a surface with spiky peaks at each kernel center, while setting it too large creates humps with maxima that are not necessarily located at the kernel center. However, for the case of the triweight kernel function, one can guarantee an *N*-modal function by setting the smoothing parameter to 95% of the minimum Euclidean distance between any two kernel centers.

The KDE method is used to create three multimodal functions that are scaled from one through ten dimensions (i.e., one through ten independent variables). In the first scenario, there are $N = 2$ kernels (modes) regardless of the dimensionality of the problem. In the second scenario, there are $N = D$ kernels, i.e. the number of modes is equal to the number of independent variables. Lastly, in the third scenario, there are $N = 2D$ kernels and the number of modes is always equal to twice the number of independent variables. Posing the problem in this way creates a unique challenge for the metamodeling methods. Specifically, the effect of scaling the number of independent variables can be investigated directly for different levels of modality.

Fig. 1b. Hot and cold stream temperature profiles. (Mills, 1998)

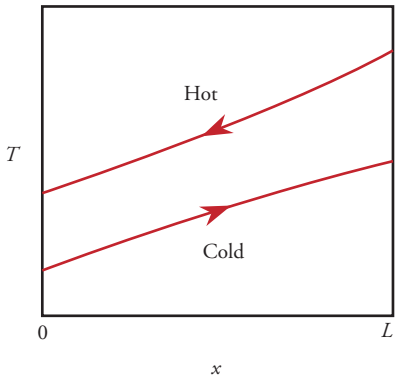

Two Stream Counter-Flow Heat Exchanger

In addition to the functions generated using the KDE method, a two stream, counter-flow shell and tube heat exchanger, such as that used in a shipboard freshwater cooling loop, is used as an example function. A schematic of this type of heat exchanger is shown in Fig. 1a. The heat exchanger features a bundle of conductive tubes inside a cylindrical shell. The hot and cold streams flow in opposite directions resulting in temperature profiles similar to those shown in Fig. 1b. The working fluid in the hot and cold streams is assumed to be fresh liquid water. The temperature dependence of the fluid properties is not ignored, and the outer surface of the shell is assumed to be adiabatic.

The output of this model is the overall heat transfer rate from the hot stream to the cold stream. This response, given by (16), is obtained by multiplying the maximum theoretical heat transfer rate by the heat exchanger effectiveness ε:

$$\dot{Q} = \varepsilon \dot{Q}_{max} = \frac{1 - e^{-N_{tu}(1+R_C)}}{1 + R_C} \tag{16}$$

where

$$R_C = \frac{C_{min}}{C_{max}} = \frac{\min(\dot{m}_H C_{p,H}, \dot{m}_C C_{p,C})}{\max(\dot{m}_H C_{p,H}, \dot{m}_C C_{p,C})} \tag{17}$$

and

$$N_{tu} = \frac{UA}{C_{min}} \tag{18}$$

In (17), $\dot{m}_h$ and $\dot{m}_c$ are the mass flow rates of the hot and cold streams in the heat exchanger, respectively. The $C_{p,h}$ and $C_{p,c}$ terms refer to the specific heats of the hot and cold streams, respectively. In (18), *UA* is the overall heat transfer coefficient between the two fluids and is calculated using a combination of conductive and convective heat transfer equations *(Mills, 1998)*. Lastly, the maximum theoretical heat transfer rate is given by (19):

$$\dot{Q}_{max} = C_{min}(T_{H,in} - T_{C,in}) \tag{19}$$

where $T_{H,in}$ and $T_{C,in}$ are the hot stream and cold stream inlet temperatures, respectively. A thorough explanation and derivation of this heat exchanger model is provided in *(Mills, 1998)*.

Ten independent variables from the above heat exchanger model are selected for this study. The variables and response are listed in Table 1, along with their respective symbols and units. The variables listed in Table 1 are self explanatory with the exception of the flow area ratio. This variable is the ratio of the cross sectional area of the fluid flowing through the shell to the total shell area. It is an indicator of how tightly packed the tubes are within the shell.

To create the one through ten variable test problems that are used in this study, variables are added one at a time in the order listed in Table 1. The variables whose main effects have the most curvature are added last in an effort to exploit weaknesses of any particular method in high dimensional space.

Table 1. Heat exchanger model response and independent variables

Model Response			
Response	*Symbol*	*Units*	
Overall heat transfer rate		W	
Model Variables			
Variable	*Symbol*	*Units*	*Main Effect*
Cold stream inlet temperature	$T_{C,in}$	K	Quasi-Linear
Hot stream inlet temperature	$T_{H,in}$	K	Quasi-Linear
Tube thickness	T	m	Quasi-Linear
Flow Area Ratio	A_r	n/a	Quasi-Linear
Tube fouling heat resistance	R_f	m^2K/W	Quasi-Linear
Cold stream flow rate	$\dot{m}_C$	kg/s	Exponential
Hot stream flow rate	$\dot{m}_H$	kg/s	Exponential
Shell length	L	m	Exponential
Number of tubes	N	Integer	Exponential
Tube inner diameter	D	m	Quasi-Quadratic

Experimental Design

Training and Test Point Sampling Strategy

The method for sampling training points from the base model can have a significant effect on the accuracy of the resulting metamodel. In contrast to physical experiments, which are stochastic in nature, deterministic computer models are not subjected to repeated sampling because their predictions typically do not vary unless the input variables change. Therefore, sampling strategies for computer experiments aim to fill the design space as uniformlyas possible *(Koehler and Owens, 1996)*. There are several so-called space filling designs such as Latin hypercube designs *(Mckayet al., 1979)*, Hammersley sequence sampling *(Hammersley, 1960)*, orthogonal arrays *(Owen, 1992)*, and uniform designs *(Fang et al., 2000)*.

Simpson et al. *(Simpson et al., 2002)* find that uniform designs and Hammersley sequence

sampling tend to fill the design space more evenly and provide more accurate results than Latin hypercube designs and orthogonal arrays. They also show that Hammersley sequencing is preferred to uniform designs when large sets of training data can be afforded. In contrast to an expensive computer simulation, all of the test functions used in this paper can be sampled rapidly and large sets of training data are available. Therefore, Hammersley sequence sampling is selected as the method for generating training and test points in this study.

Performance Assessment

In this study, the metamodeling techniques are evaluated based on the number of training points needed to achieve a predetermined error metric. The error metric used is the relative average absolute error (RAAE) and is given by (20):

$$RAAE = \frac{\sum_{i=1}^{n} |y - \hat{y}_i|}{n\sigma} \qquad (20)$$

where y_i is the actual value of the base model at the i_{th} test points, $\hat{y}_i$ is the predicted value from the metamodel, n is the number of sample points, and σ is the standard deviation of the response.

To determine the requirednumber of training points, the quantity of training points is increased continuously until an *RAAE* value of 0.25 is achieved. The training points are generated with Hammersley sequence sampling. The *RAAE* is calculated using one hundred test points per variable (100D), which are also generated with a Hammersley sequence.

One issue with this testing strategy is the possibility that some of the training points and test points overlap. For example, in the 1D case, all of the training points will overlap with test points if the number of test points is divisible by the number of test points. Overlapping is to be avoided because testing interpolating methods (kriging and RBF) at the trainingpoints results in zero error. To avoid overlapping in the 1D problem, 101 test points (a prime number) are used. In higher dimensions, test points and training points do not overlap in a Hammersley sequence provided that the number of training points does not equal the number test points.

In addition to the number of sample points necessary to achieve the pre-specified error metric, the computational times required to build each model and to predict the 100D test points are also recorded. All experiments are performed on a 32-bit PC with an Intel Pentium® Dual-Core 2.50 GHz processor with 4.00 GB of RAM.

Table 2. Complete experimental plan

Tests Performed				
Test	*Test Function*	*Scale*	*Test Points*	*Termination Criteria*
1	2 mode kernel	1-10D	100*D (101 in 1D)	RAAE < 0.25
2	D mode kernel			
3	2D mode kernel			
4	Heat Exchanger			

Table 2 includes a summary of the tests to be performed. Metamodels are created in one through ten dimensions for the heat exchanger model and three kernel density estimation functions of varying modality. Performing this task with all three of the metamodeling methods results in a total of 120 tests.

Results and Discussion

Graphical representations of the results of the study are provided in Figs. 2 to 5. In each figure, the abscissa indicates the dimensionality of each problem, while the ordinate represents the number of training points required to meet the error threshold of *RAAE* <0.25. The center of each circle represents the number of training points required for the specific dimension and metamodeling method. The size of the solid circles represents the relative training time for each metamodel and the translucent circles represent the relative prediction

time for 100D new data points. A complete tabulation of the numerical results is provided in Appendix A.

Fig. 2. N = 2 mode KDE results

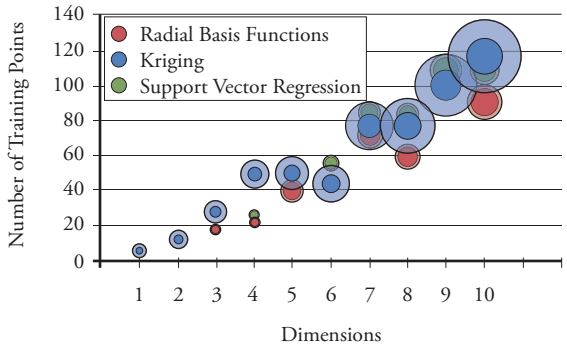

Fig. 3. N = D mode KDE results

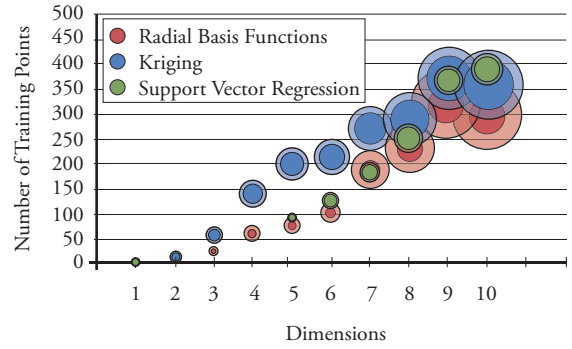

Fig. 4. N = 2D mode KDE results

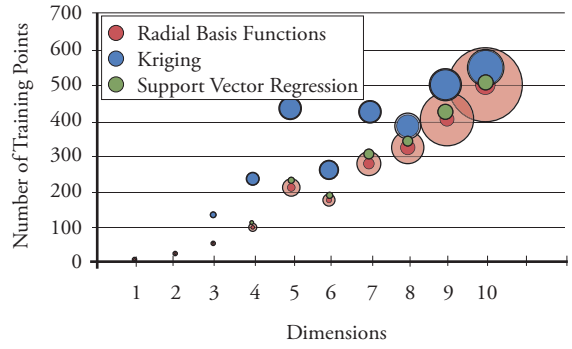

Required Number of Training Points

For all three of the kernel based functions, the general trend is that the required number of training points scales linearly with the number

Fig. 5. Heat exchanger model

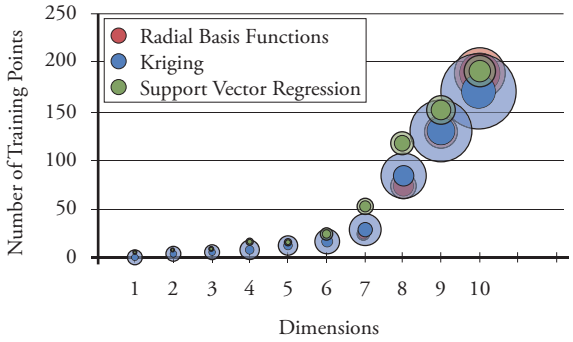

of dimensions. Also, the functions with higher modality require a higher number of training points. In most cases, radial basis function metamodels require the smallest number of training points of the three methods, followed by support vector regression. Kriging metamodels tend to need the highest number of training points of all.

The ability of radial basis functions and support vector regression to model the base functions with few training points can be attributed partially to careful selection of user-defined tuning parameters. Recall from equations (6) and (10) that the Gaussian basis and kernel functions contain tuning parameters k and g for radial basis functions and support vector regression, respectively. The value of these parameters has a significant effect on the quality of the resulting metamodel fit. In this study, these parameters were selected by trial and error until optimal values were obtained. Kriging, on the other hand, has correlation parameters θ_i that are identified automatically during the fitting process. This automated identification of the correlation parameters is effective but requires significant computational expense.

The results of the heat exchanger are slightly different than those of the kernel function. The required number of training points to model the heat exchanger in most dimensions is very similar for kriging and radial basis functions, with support vector regression needing only slightly more in a few cases. Generally speaking, all methods are able to

approximate the heat exchanger model accurately with very few training points when compared to the highly modal and nonlinear function produced using the kernel density estimation method. For the heat exchanger model, the required number of training points increases sharply after 6 dimensions. This result is expected because the variables with the most nonlinear effects are added to the model last, as explained in section 3.2.

Training and Prediction Time

Training and prediction times are represented qualitatively in Figs. 2 – 5 by the size of the solid and translucent circles, respectively. The general trend in all four cases is that the training and prediction times of all methods increase with the number of dimensions. Support vector regression has the smallest training times in all cases. Kriging is slightly slower than radial basis functions when applied to low modality problems in low dimensions. Training times for radial basis functions become very large compared to kriging when applied to high modality, high dimensional problems. The theory behind support vector regression is very computationally efficient *(Clarke et al., 2005)*, and other comparison studies have confirmed its low training times *(Ely and Seepersad, 2009)*. Build times for kriging are expected to be slow because it must perform a nonlinear optimization to obtain the correlation parameters. The slow training times for radial basis functions in highly nonlinear, multidimensional problems stems from the large number of training points required to train an accurate model. During the build process, the RBF method must compute Euclidean distances between adjacent training points. The number of these calculations increases dramatically when the number of dimensions and training points is large.

The manner in which the training times increase with dimensions also varies among the metamodeling methods. The training times for kriging appear to increase linearly with the scale of the problem, but the training times for RBF and SVR begin to increase sharply in the higher dimensional problems. If this trend were extended into very high dimensions, it is possible that the training times for SVR may actually approach or exceed those of kriging.

Support vector regression is also seen to have by far the smallest prediction times of the three methods studied. This trend is also consistent with previous studies *(Clarke et al., 2005; Ely and Seepersad, 2009)*. Kriging has the slowest prediction times of the three methods, being as much as ten times larger than radial basis functions in some cases. Kriging and radial basis function are expected to have large prediction times because the distances between points must be computed during the simulation process *(Jin et al., 1999)*.

Prediction time not only depends on the method used and the scale of the problem, but also on the type of problem being modeled. Even though the number of test points is the same for each respective dimension of each problem, the prediction time increases with the modality of the problem. That is, it takes a given method longer to predict 1000 new points for a more complex problem than it does for a simple one.

Conclusions

In this paper, three types of metamodels—kriging, radial basis functions, and support vector regression—are compared with respect to their speed, accuracy, and required number of training points for test problems of varying complexityand dimensionality. Radial basis functions are found to model and predict the test functions to a predetermined level of global accuracy with the smallest number of training points for most functions. In most cases, kriging metamodels need the highest number of training points of the three methods. Kriging has faster model building times than radial basis functions, but it is slower to predict new data points. Both methods are very slow to train and predict new points when compared to support vector regression.

Metamodel-based optimization has numerous potential applications in the field of marine engineering and ship design. Building ship

prototypes and conducting full scale physical experiments are often too expensive or time consuming to be practical in the early stages of the design process, thus driving the need for complex computer models. Using metamodels in place of computationally expensive computer models and simulations can drastically reduce design time and enable ship designers to explore larger regions of the feasible design space.

Acknowledgements

The authors would like to thank the Office of Naval Research (ONR) for supporting this work under the auspices of the Electric Ship Research and Development Consortium. The guidance and experience offered by Dr. Tom Kiehne of Applied Research Laboratories are also gratefully acknowledged.

References

BOX, G. E. P. and K. B. WILSON, 1951, *"On the Experimental Attainment of Optimal Conditions,"* Journal of the Royal Statistical Society, Vol. 13, pp. 1-45.

CLARKE, S. M., J. H. GRIEBSCH and T. W. SIMPSON, 2005, *"Analysis of Support Vector Regression for Approximation of Complex Engineering Analysis,"* Journal of Mechanical Design, Vol. 127, pp. 1077-1087.

DIMOPOULOS, G. G., A. V. KOUGIOUFAS and C. A. FRANGOPOULOS, 2008, *"Synthesis, Design, and Operation Optimization of a Marine Energy System,"* Energy, Vol. 33, pp. 180-188.

ELY, G. R. and C. C. SEEPERSAD, 2009, *"A Comparative Study of Metamodeling Techniques for Predictive Process Control of Welding Applications,"* ASME International Manufacturing Science and Engineering Conference, West Lafayette, Indiana, USA, Paper Number MESC2009-84189.

FANG, H., M. RAIS-ROHANI, Z. LIU and M. F. HORSTMEYER, 2005, *"A Comparative Study of Metamodeling Methods for Multiobjective Crashworthiness Optimization,"* Computers and Structures, Vol. 83, pp. 2121-2136.

FANG, K. T., D. K. J. LIN, P. WINKER and Y. ZHANG, 2000, *"Uniform Design: Theory and Applications,"* Technometrics, Vol. 42, No. 3, pp. 237-248.

FRIEDMAN, J. H., 1991, *"Multivariate Adaptive Regression Splines,"* The Annals of Statistics, Vol. 19, No. 1, pp. 1-67.

GIUNTA, A. and L. T. WATSON, 1998, *"A Comparison of Approximation Modeling Techniques: Polynomial Versus Interpolating Models,"* 7th AIAA/USAF/ISSMO Symposium on Multidisciplinary Analysis & Optimization, St. Louis, MO, AIAA, Vol. 1, pp.392-404. AIAA-98-4758.

HAMMERSLEY, J. M., 1960, *"Monte Carlo Methods for Solving Multivariable Problems,"* Annals of the New York Academy of Sciences, Vol. 86, pp. 844-874.

HARDY, R. L., 1971, *"Multiquadric Equations of Topology and Other Irregular Surfaces,"* Journal of Geophysical Research, Vol. 76, No. 8, pp. 1905-1915.

HAYKIN, S., 1999, Neural Networks: A Comprehensive Foundation, Prentice Hall, Upper Saddle River, N.J.

JIN, R., W. CHEN and T. W. SIMPSON, 2001, *"Comparative Studies of Metamodeling Techniques Under Multiple Modeling Criteria,"* Structural and Multidisciplinary Optimization, Vol. 23, pp. 1-13.

KIM, B.-S., Y.-B. LEE and D.-H. CHOI, 2009, *"Comparison Study on the Accuracy of Metamodeling Technique for Non-Convex Functions,"* Journal of Mechanical Science and Technology, Vol. 23, pp. 1175-1181.

KOEHLER, J. R. and A. B. OWENS, 1996, *"Computer Experiments,"* Handbook of Statistics, Elsevier Science, New York, Vol. 13, pp. 261-308.

LEE, Y., S. OH and D.-H. CHOI, 2008, *"Design Optimization Using Support Vector Regression,"* Journal of Mechanical Science and Technology, Vol. 22, pp. 213-220.

MCKAY, M. D., R. J. BECKMAN and W. J. CONOVER, 1979, *"A Comparison of Three Methods for Selecting Values of Input Variables in the Analysis of Output from a Computer Code,"* Technometrics, Vol. 21, No. 2, pp. 239-245.

MILLS, A. F., 1998, Heat Transfer, Prentice Hall, Upper Saddle River, NJ.

OWEN, A. B., 1992, "*Orthogonal Arrays for Computer Experiments, Integration, and Visualization,"* Statistica Sinica, Vol. 2, pp. 439-452.

PARZEN, E., 1962, *"On Estimation of a Probability Density Function and Mode,"* The Annals of Mathematical Statistics, Vol. 33, No. 3, pp. 1065-1076.

PERCIVAL, S., D. HENDRIX and F. NOBLESSE, 2001, *"Hydrodynamic Optimization of Ship Hull forms,"* Applied Ocean Research, Vol. 23, pp. 337-355.

PERI, D., M. ROSSETTI and E. F. CAMPANA, 2001, "Design Optimization of Ship Hulls via CFD Techniques," Journal of Ship Research, Vol. 45, No. 2, pp. 140-149.

RACINE, B. J. and E. G. PATERSON, 2005, *"CFD-Based Method for Simulation of Marine-Vehicle Maneuvering,"* 35th AIAA Fluid Dynamics Conference and Exhibit, Toronto, Ontario Canada.

SACKS, J., S. B. SCHILLER and W. J. WELCH, 1989, *"Designs for Computer Experiments,"* Technometrics, Vol. 31, No. 1, pp. 41-47.

SCOTT, D. W., 1992, Multivariate Density Estimation, John Wiley & Sons, Inc., New York.

SIMPSON, T., L. DENNIS and W. CHEN, 2002, *"Sampling Strategies for Computer Experiments: Design and Analysis,"* International Journal of Reliability and Application, Vol. 2, No. 3, pp. 209-240.

SIMPSON, T. W., T. M. MAUERY, J. J. KORTE and F. MISTREE, 1998, *"Comparison of Response Surface and Kriging Models for Multidisciplinary Design Optimization,"* 7th AIAA/USAF/NASA/ISSMO Symposium on Multidisciplinary Analysis and Optimization, Vol. 1, pp. 381-391.

VAPNIK, V., S. GOLOWICH and A. SMOLA, 1997, *"Support Vector Method for Function Approximation, Regression Estimation, and Signal Processing,"* Advances in Neural Information Processing Systems, Vol. 9, pp. 281-287.

WANG, X., Y. LIU and E. K. ANTONSSON, 1999, *"Fitting Functions to Data in High Dimensionsal Design Space,"* ASME Design Engineering Technical Conferences, Las Vegas, NV, Paper Number DETC99/DAC-8622.

WATANABE, T., T. KAWAMURA, Y. TAKEKOSHI, M. MAEDA and S. H. RHEE, 2003, *"Simulation of Steady and Unsteady Cavitation on a Marine Propeller Using a RANS CFD Code,"* Fifth International Symposium on Cavitation, Osaka, Japan.

Application of Sampling Based Model Predictive Control to an Autonomous Underwater Vehicle

Aplicación de Muestreo basado en Modelos de Control Predictivo a un Vehículo Autónomo Subacuático

Charmane V. Caldwell[1]
Damion D. Dunlap[2]
Emmanuel G. Collins Jr.[3]

Abstract

Unmanned Underwater Vehicles (UUVs) can be utilized to perform difficult tasks in cluttered environments such as harbor and port protection. However, since UUVs have nonlinear and highly coupled dynamics, motion planning and control can be difficult when completing complex tasks. Introducing models into the motion planning process can produce paths the vehicle can feasibly traverse. As a result, Sampling-Based Model Predictive Control (SBMPC) is proposed to simultaneously generate control inputs and system trajectories for an autonomous underwater vehicle (AUV). The algorithm combines the benefits of sampling-based motion planning with model predictive control (MPC) while avoiding some of the major pitfalls facing both traditional sampling-based planning algorithms and traditional MPC. The method is based on sampling (i.e., discretizing) the input space at each sample period and implementing a goal-directed optimization (e.g., A*) in place of standard numerical optimization. This formulation of MPC readily applies to nonlinear systems and avoids the local minima which can cause a vehicle to become immobilized behind obstacles. The SBMPC algorithm is applied to an AUV in a 2D cluttered environment and an AUV in a common local minima problem. The algorithm is then used on a full kinematic model to demonstrate the benefits.

Key words: Motion planning, path planning, model predictive control, sampling, autonomous underwater vehicles.

Resumen

Los UUVs pueden ser utilizados para realizar tareas difíciles en ambientes atiborrados de reflexiones de onda tales como muelles y puertos. Sin embargo, dado que los UUVs tienen dinámicas áltamente acopladas y no lineales, la programación de movimiento y el control pueden ser complicados cuando son realizadas tareas complejas. Introducir modelos en el proceso de programación del movimiento puede producir patrones que el vehículo puede cruzar de manera viable. Como resultado, el modelo de control predictivo basado en muestreo (SBMPC, por sus siglas en inglés) es propuesto para generar simultáneamente entradas de control y trayectorias de sistema para un vehículo autónomo sumergible. El algoritmo combina los beneficios de la planeación de movimiento con el control predictivo de modelo (MPC), mientras que evita algunos de los mayores obstáculos que enfrentan tanto los algoritmos basados en muestreo como el tradicional MPC. El método está basado en el muestreo (es decir, discretización) del espacio de entrada en cada período de muestreo e implementación de una optimización dirigida a objetivos (por ejemplo, A*) en lugar de la optimización numérica estándar. Esta formulación del MPC aplica fácilmente a los sistemas no lineales y evita el mínimo local, el cual puede ocasionar que un vehículo quede inmóvil detrás de los obstáculos. El algoritmo SBMPC se aplica a un UAV en un ambiente cargado de reflexiones de onda y a un UAV en un problema de mínimo común local. El algoritmo es luego usado en un modelo cinemático completo para demostrar los beneficios de aplicar restricciones y un modelo en programación de movimiento.

Palabras claves: Programación de movimiento, programación de ruta, Modelo de control predictivo, muestreo, Vehículo Autónomo Subacuático.

Date received: May 21th, 2010. - *Fecha de recepción: 21 de Mayo de 2010.*
Date Accepted: July 6, 2010. - *Fecha de aceptación: 6 de Julio de 2010.*

[1] Department of Electrical and Computer Engineering CISCOR of the FAMU-FSU COE. Florida. U.S.A. e-mail: cvcaldwe@eng.fsu.edu
[2] Naval Surface Warfare Center. Panama City, FL. U.S.A. e-mail: damion.d.dunlap@navy.mil
[3] Department of Electrical and Computer Engineering CISCOR of the FAMU-FSU COE. Florida. U.S.A. e-mail: ecollins@eng.fsu.edu

Introduction

The United States has over 360 ports that comprise more than 90% of the U.S. export and import industry [1]. These harbors pass through cargo and even passengers. A threat to the ports can produce an environmental and economic crisis [2]. A simple tactic a terrorist can use to cause havoc is employing mines or maritime improvised explosive devices (MIEDs) at a U.S. port. In this way a mine that cost no more than a few thousand dollars can cause great disruption. There have been non-mine related crises in the past that have caused setbacks at U.S. ports: the Exxon Valdez spill of 1989, which cost more than $2.5 billion to clean up, and the dock workers strike of 2002, which resulted in a loss of $1.9 billion dollars a day [2]. The effect of closing a port due to a mine explosion can also be catastrophic.

Consequently, it is necessary to protect U.S. ports. The task of searching and destroying mines is a dangerous process that can be performed by a combination of surface vehicles, unmanned underwater vehicles (UUVs), and explosive ordinance divers (EODs) [1]. This paper will consider the use of an UUV, more specifically an autonomous underwater vehicle (AUV). Harbors and ports have naval ships, commercial vessels, fishing boats, piers and other articles that create a cluttered environment for AUV motion. For the inspection to be successful the AUV cannot collide with an obstacle, because this can obviously be very disruptive. In addition to the complex AUV mobility environment, the nonlinear, timvarying and highly coupled vehicle dynamics make motion planning and control difficult for harbor protection tasks since it is difficult to predict future paths for the vehicle as it moves through the environment. In addition, there are uncertainties in the hydrodynamic coefficients determined in a tank test, which effect the confidence in the fidelity of the dynamic model when the AUV maneuvers in the ocean. The vehicle is underdamped and easily perturbed, which is a challenge when there are external disturbances like ocean currents that cause the vehicle to deviate from its path. Furthermore, the center of gravity and buoyancy may change depending on the AUV payload. Consequently, an AUV requires robust motion planning and control to operate reliably in complex environments.

Standard AUV motion planning and control first determines a trajectory that the AUV may not be physically able to follow, then applies a controller that may require the vehicle to follow this possibly infeasible trajectory. An approach that can help ensure robust motion planning is to incorporate a model of the AUV when planning the vehicle trajectory since this applies motion constraints that ensure feasible trajectories. In cluttered environments, the use of kinodynamic constraints in motion planning aid in determining a collision free trajectory. The kinematics provides the turn rate constraint and side slip [3], while the dynamics can provide insight into an AUV's movement and interaction with the water, providing limits on velocities, accelerations and applied forces. This paper presents results for motion planning with a kinematic model. A future paper will consider planning using an AUV dynamic model.

There are researchers that have previously incorporated a model in motion planning for an AUV. Kawano has a four part system [4]: 1) the offline Markov Decision Process module performs the motion planning offline; 2) the replanning module determines a path when there are new obstacles; 3) the realtime path tracking module gives action that needs to be taken; 4) the feedback control module regulates the vehicles' velocity to the target velocity. Yakimenko uses the direct method of calculus to generate trajectories that are kinematically feasible for the vehicle to traverse [5]. There are four main blocks: the first generates a candidate trajectory that satisfies boundary conditions and position, velocity and acceleration constraints; the second employs inverse dynamics to determine the states and control inputs necessary to follow the trajectory; the third computes states along the reference trajectory over a fixed number of points; and the fourth optimizes the performance index.

The current line of research first considered using the model in the motion planning process by

integrating the guidance and control via a method called shrinking horizon model predictive control [6]. That approach was often able to determine a collision free path using a kinematic model, but had two primary shortcomings. First, the computational time was not fast enough for real time vehicle operation. Second, for certain initial condition the gradient-based optimization method would converge to a local minimum. To solve these issues Sampling Based Model Predictive Control (SBMPC) was developed [7].

SBMPC allows a model to be considered online while simultaneously determining the optimal control input and a kinematically or dynamically feasible trajectory of the AUV. SBMPC is a nonlinear model predictive control (NMPC) algorithm that can avoid local minimum, has strong convergence properties based on the *LPA** optimization convergence proof [8], and has physically intuitive tuning parameters. The concept behind SBMPC was first presented in [7]. A more developed version that tested SBMPC on an Ackerman Steered vehicle [9] was later presented. As its name implies, SBMPC is dependent upon the concept of sampling, which has arisen as one of the major paradigms for robotic motion planning [10]. Sampling is the mechanism used to trade performance for computational efficiency. Unlike traditional model predictive control (MPC), which views the system behavior through the system inputs, the vast majority of previously developed sampling methods plan in the output space and attempt to find inputs that connect points in the output space. SBMPC is an algorithm that, like traditional MPC, is based on viewing the system through its inputs. However, unlike previous MPC methods, it uses sampling to provide the trade-off between performance and computational efficiency. Also, in contrast to previous MPC methods, it does not rely on numerical optimization. Instead it uses a goal-directed optimization algorithm derived from *LPA** [8], an incremental *A** algorithm [10].

This paper is arranged as follows. Section II provides a summary of the methods combined to formulate SBMPC. The SBMPC algorithm is presented in Section III. Section IV gives two-dimensional simulations of SBMPC implemented on AUVs in clustered environments and local minima configurations. Then a three-dimensional simulation in free space is provided. Finally, Section V presents conclusions and future work.

The Fundamentals of Sampling Based Model Predictive Control

SBMPC is a novel approach that allows real time motion planning that uses the vehicle's nonlinear model and avoids local minima. The method employs an MPC type cost function and optimizes the inputs, which is standard in the control community. Instead of using traditional numerical optimization, SBMPC applies sampling and a goal-directed (*A**-type) optimization, which are standard in the robotic and AI communities. This section provides a brief overview of the methods from which SBMPC was derived. Next, it describes the SBMPC cost function and outlines the SBMPC algorithm. Finally, this section disusses the benefits of SBMPC.

Model Predictive Control

Introduced to the process industry in the late 1970s [11], Model Predictive Control (MPC) is a mixture of system theory and optimization. It is a control method that finds the control input by optimizing a cost function subject to constraints. The cost function calculates the desired control signal by using a model of the plant to predict future plant outputs. MPC generally works by solving an optimization problem at every time step k to determine control inputs for the next N steps, known as the prediction horizon. This optimal control sequence is determined by using the system model to predict the potential system response, which is then evaluated by the cost function J. Most commonly, a quadratic cost function minimizes control effort as well as the error between the predicted trajectory and the reference trajectory, r. The prediction and optimization operate together to generate sequences of the controller output u and the resulting system output y. In particular, the optimization problem is

$$\min J = \sum_{i=1}^{N} \left\| r(k+i) - y(k+i) \right\|_Q^2 + \sum_{i=1}^{M-1} \left\| \Delta u(k+i) \right\|_S^2 \quad (1)$$

subject to the model constraints,

$$x(k+i) = f(x(k+i-1), u(k+i-1)), \quad (2)$$

$$x(k+i) = g(x(k+i-1)), \quad (3)$$

and the inequality constraints,

$$\begin{aligned} Ax &\le b \\ C(x) &\le 0 \\ u^l \le u(k+i) &\le u^u \end{aligned} \quad (4)$$

Traditional MPC has typically been computationally slow and incorporates simple linear models.

Sampling Based Motion Planning

Sampling-based motion planning algorithms include Rapidly-exploring Random Tree (RRTs) [12], probability roadmaps [13], and randomized *A** algorithms [14]. A common feature of each of those algorithms to date is that they work in the output space of the robot and employ various strategies for generating samples (i.e., random or pseudo-random points). In essence, as shown in Fig. 1, sampling-based motion planning methods work by using sampling to construct a tree that connects the root with a goal region. The general purpose of sampling is to cover the space so that the samples are uniformly distributed, while minimizing gaps and clusters [15].

Fig. 1. A tree that connects the root with a goal region

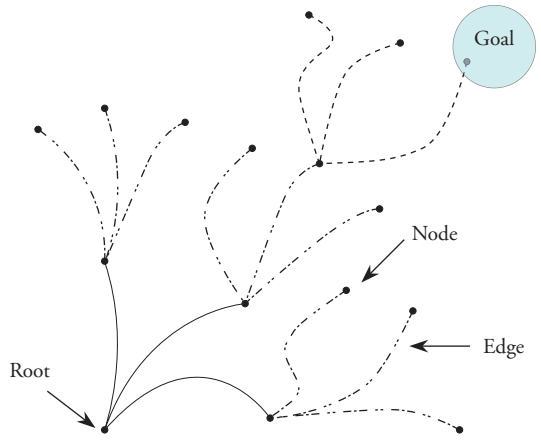

Goal Directed Optimization

There is a class of discrete optimization techniques that have their origin in graph theory and have been further developed in the path planning literature. In this paper these techniques will be called *goal-directed optimization* and refer to graph search algorithms such as Dijkstra's algorithm and the *A**, *D**, and *LPA** algorithms [10], [8]. Given a graph, these algorithms find a path that optimizes some cost of moving from a start node to some given goal. Although not commonly recognized, goal-directed optimization approaches are capable of solving control problems for which the ultimate objective is to generate an optimal trajectory and control inputs to reach a goal (or set point) while optimizing a cost function; hence, they apply to terminal constraint optimization problems and set point control problems.

The SBMPC Optimization Problem

SBMPC overcomes some of the shortcomings of traditional MPC by sampling the input space as opposed to sampling the output space as in traditional sampling-based motion planning methods. The need for a nearest-neighbor search is eliminated and the local planning method (LPM) is reduced to the integration a system model and therefore only generates outputs that are achievable by the system. To understand the relationship between sampling-based algorithms and MPC optimization, it is essential to pose sampling-based motion planning as an optimization problem. To illustrate this point, note that, *subject to the constraints of the sampling*, a goaldirected optimization algorithm can effectively solve the mixed integer nonlinear optimization problem,

$$\min_{\{u(k),\ldots,u(k+N-1)\},N} J = \sum_{i=0}^{N} \left\| y(k+i+1) - y(k+i) \right\|_{Q(i)} + \sum_{i=1}^{N-1} \left\| \Delta u(k+i) \right\|_{S(i)} \quad (5)$$

subject to the system equations,

$$x(k+i) = f(x(k+i-1), u(k+i-1)), \quad (6)$$

$$x(k) = g(x(k)), \quad (7)$$

and the constraints,

$$\|y(k+i) - \mathbf{G}\| \leq \epsilon, \quad (8)$$

$$x(k+i) \in \mathbf{X}_{free} \ \forall \ i \leq N, \quad (9)$$

$$u(k+i) \in \mathbf{U}_{free} \ \forall \ i \leq N, \quad (10)$$

where $\Delta u(k+i) = u(k+i) - u(k+i-1)$, $Q(i) \geq 0$, $S(i) \geq 0$, and $\mathbf{X}_{free}$ and $\mathbf{U}_{free}$ represent the states and inputs respectively that do not violate any of the problem constraints. The term $\|y(k+i+1) - y(k+i)\|_{Q(i)} + \|\Delta u(k+i)\|_{S(i)}$ represents the edge cost of the path between the current predicted output $y(k+i)$ and the next predicted output $y(k+i+1)$. The goal state G is represented as a terminal constraint as opposed to being explicitly incorporated into the cost function. Goal-directed optimization methods implicitlyconsider the goal through the use of a function that computes a rigorous lower bound of the cost from a particular state to G. This function, often referred to as an "optimistic heuristic" in the robotics literature, is eventually replaced by actual cost values based on the predictions and therefore does not appear in the final cost function. The cost function can be modified to minimize any metric as long as it can be computed as the sum of edge costs.

The SBMPC ALGORITHM

The formal SBMPC algorithm can be found in [9]. However, the main component of the SBMPC algorithm is the optimization, which will be called Sampling-Based Model Predictive Optimization and consists of the following steps:

1. ***Sample Control Space:*** Generate a set of samples of the control space that satisfy the input constraints.
2. ***Generate Neighbor Nodes:*** Integrate the system model with the control samples to determine the neighbors of the current node.
3. ***Evaluate Node Costs:*** Use an *A**-like heuristic to evaluate the cost of the generated nodes based on the desired objective (shortest distance, shortest time, or least amount of energy, etc.).
4. ***Select Lowest Cost Node:*** The nodes are collected in the Open List, which ranks the potential expansion nodes by their cost. The Open List is implemented as a heap so that the lowest cost node that has not been expanded is on top.
5. ***Evaluate Edge Cost for the "Best" Node:*** Evaluate each of the inequality constraints described in (6) for the edge connecting the "best" node to the current node. The edge cost evaluation requires sub-sampling and iteration of the model with a smaller time step for increased accuracy; it is therefore only computed for the current "best"node. In the worst case the edge cost of all of the neighbor nodes will be evaluated, which is how *A** typically computes cost.
6. ***Check for Constraint Violations:*** If a constraint violation occurred, go back to step 4 and get the next "best" node.
7. ***Check for Completion:*** Determine if the current solution contains a path to the goal. If yes, stop. If no, go back to step 1.

The entire algorithm is integrated into the MPC framework by executing the first control and repeating the optimization until the goal is reached since the completion of SBMPO represents the calculation of a path to the goal and not the complete traversal.

Benefits of SBMPC

The novel SBMPC approach has several benefits. First, SBMPC is a method that can address problems with nonlinear models. It effectively reduces the problem size of MPC by sampling the inputs of the system, which considerably reduces the computation time. In addition, the method also replaces the traditional MPC optimization phase with *LPA**, an algorithm derived from *A** that can replan quickly (i.e., it is incremental). SBMPC retains the computational efficiency and has the convergence properties of *LPA** [8], while avoiding some of the computational bottlenecks

associated with sampling-based motion planners. Lastly, tuning for this method requires choosing the number of samples and the implicit state grid resolution, which are physically intuitive parameters.

SBMPC Simulation Results

The results presented in this section have three purposes:
1) to demonstrate how SBMPC can handle AUVs moving in cluttered environments, 2) to demonstrate how the SBMPC algorithm behaves when a local minimum is present and the effect sampling has on the optimal solution, and 3) to show how the inclusion of constraints and a model in motion planning can produce a feasible path. It is assumed the obstacle information is available to the SBMPC algorithm. The problems associated with the uncertainty in sensing obstacles are beyond the scope of this paper. However, it must be addressed for real world implementation of SBMPC on AUVs.

SBMPC Motion Planning for an AUV in Cluttered Environments

Motion planning for an AUV moving in the horizontal plane is developed using the 2-D kinematic model,

$$\begin{bmatrix} \dot{x} \\ \dot{y} \\ \dot{\psi} \end{bmatrix} = \begin{bmatrix} cos\psi & 0 \\ sin\psi & 0 \\ 0 & 1 \end{bmatrix} \begin{bmatrix} u \\ r \end{bmatrix}, \qquad (11)$$

where the inputs u and r are respectively the forward velocity along the x-axis and angular velocity along the z-axis. Consequently, there are two inputs and three states in this model. The velocity u was constrained to lie in the interval (0 2) m/s, and the steering rate ψ was constrained to the interval (-15° 15°) rad/s.

The basic problem is to use the kinematic model (11) to plan a minimum-distance trajectory for the AUV from a start posture ($0m$; $0m$; 0°) to a goal point ($20m$; $20m$) while avoiding the numerous obstacles of a cluttered environment.

The parameters for the simulations are shown in Table 1. It is assumed that the time step in the SBMPC cost function (5) is T_c. For SBMPC the constraints were checked every time the model was updated (i.e., with period T_s) and $T_c > T_s$ corresponds to the period over which the control inputs were held constant. There were 100 simulations in which 30 obstacles of various sizes and locations were randomly generated to produce different scenarios. As a result, in Table 1 the prediction horizon varies because each random scenario requires a different number of steps to traverse from the start position to the goal position. In each simulation the implicit state grid resolution was 0.1m. SBMPC was used to solve the optimization problem (5) - (10) with $Q(i) = I$ and $S(i) = 0$ and yielded the optimal number of steps N^* in addition to the control input sequence.

The results of 100 random simulations on a 2 GHz Intel Core 2 Duo Laptop are shown in Table 2. Representative results from the 100 scenarios are shown in Figs. 2 and 3. These are typical scenarios which show SBMPC's ability to create a kinematically feasible trajectory in a complex environment without getting stuck in a local minimum. In the figures a circle on the path curve represents the predicted output of the vehicle that coincides with the optimal sampled input. In Fig. 2 the inputs are sampled more as the vehicle comes close to a cluster of obstacles or a large obstacle. Fig. 3 demonstrates how the AUV overcomes a large cluster of obstacles at the start of a mission. As shown in Table 2, the AUV was able to reach the goal in each of the 100 cluttered environment

Table 1. Simulation parameters

Model Time Step (Ts)	0.1s
Control Update Period (Tc)	1s
Prediction Horizon (N)	[20 47]
Control Horizon (M)	N
No. of Input Samples	10

Table 2. Simulation results.

Mean CPU Time	1.28s
Median CPU Time	0.17s
Success Rate	100%

simulations. This is important since true autonomy requires a vehicle to be able to successfully complete a mission on its own. Note there is an order of magnitude difference in the mean CPU time and median CPU time of Table 2, because a few of the randomly generated scenarios had obstacles clustered to form larger obstacles, which creates computationally intensive planning problems.

Fig. 2. Typical SBMPC clustered environment scenario in which AUV maneuvers to goal. (2-D Vehicle Path)

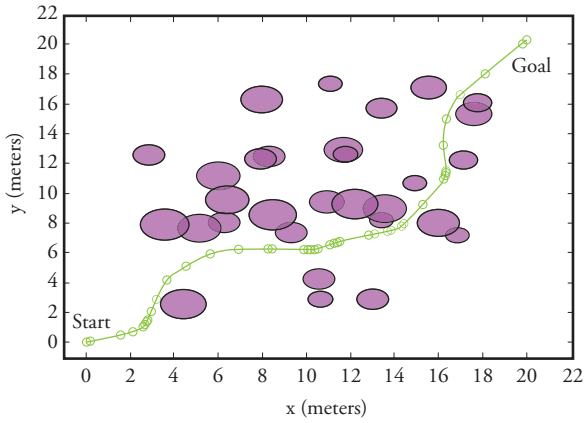

Fig. 3. Typical SBMPC clustered environment scenario in which AUV maneuvers to goal. (2-D Vehicle Path)

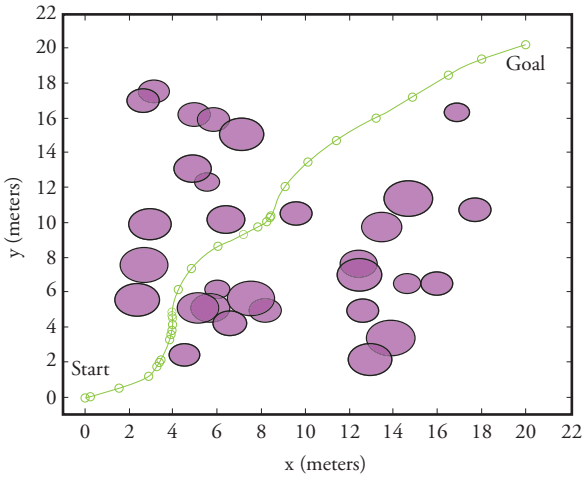

SBMPC Motion Planning for an AUV in Cluttered Environments

As stated previously, SBMPC can handle local minimum problems that other methods have difficulties handling. In this section SBMPC is used to solve a common local minimum problem in which the vehicle has a concave obstacle in front of the goal. Note that whenever the vehicle is behind an obstacle or group of obstacles and has to increase its distance from the goal to achieve the goal, it is in a local minimum position.

The parameters for these simulations are given by Table 1 with the exception that the number of samples for the simulation of Fig. 5 was increased from 10 to 25. The vehicle has a start posture of ($5m$; $0m$; 90°) and the goal position ($5m$; $10m$).

Fig. 4. A common local minimum problem where the AUV approachs a concave obstacle in front of goal with no. of input samples = 10. (2-D Vehicle Path)

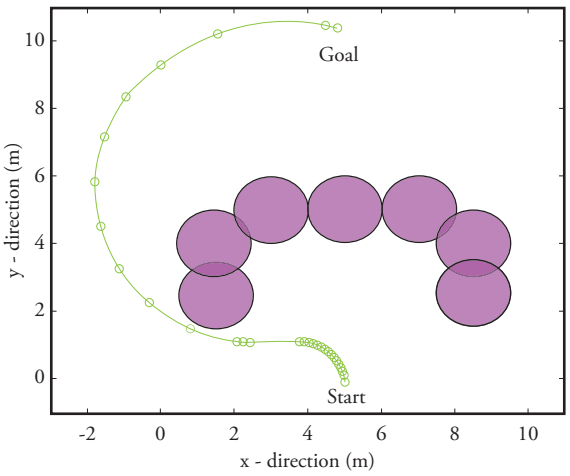

Fig. 5. A common local minimum problem where the AUV approachs a concave obstacle in front of goal with no. of input samples = 25. (2-D Vehicle Path)

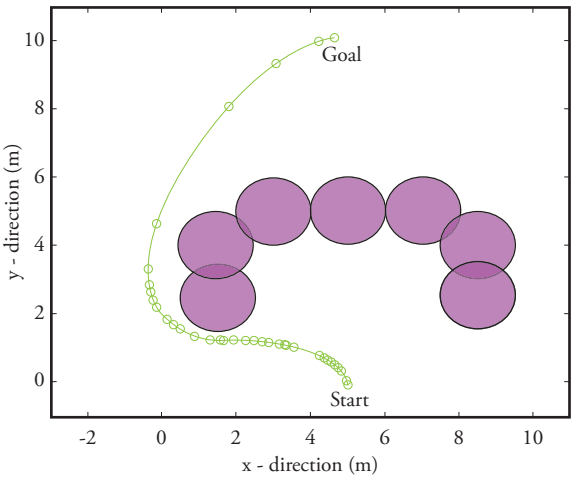

SBMPC introduces suboptimality through its sampling of the inputs. As the number of samples

of the input space increases the solution optimality increases at the expense of increased computational time. In Figs. 4 and 5 the AUVs approach the composite concave obstacle but determines a path around it to the goal. Even though, both AUVs reach the goal, because Fig. 5 uses a larger number of input samples than Fig. 4 the solution path is shorter (i.e. more optimal). This increase in the number of samples comes with a price. The path of Fig. 4, which was based on 10 samples, requires 1:0s to determine a path, but the path of Fig. 5, based on 25 input samples, has a computation time of 12:7s. To achieve an algorithm that can be implemented online there are trade offs between speed and optimality. It is important to determine a balance between the two.

SBMPC Motion Planning for an AUV in 3D Environment

Motion planning in a 3D environment uses the full kinematic model of the AUV,

$$\begin{bmatrix}\dot{x}\\ \dot{y}\\ \dot{z}\end{bmatrix} = \begin{bmatrix} c\theta c\psi & s\phi s\theta c\psi - c\phi s\psi & c\phi s\theta c\psi - s\phi s\psi \\ c\theta s\psi & s\phi s\theta s\psi - c\phi c\psi & c\phi s\theta s\psi - s\phi c\psi \\ s\theta & s\phi c\theta & c\phi c\theta \end{bmatrix}\begin{bmatrix}u\\ v\\ w\end{bmatrix}$$

$$\begin{bmatrix}\dot{\phi}\\ \dot{\theta}\\ \dot{\psi}\end{bmatrix} = \begin{bmatrix} 1 & s\phi t\theta & c\phi t\theta \\ 0 & c\phi & -s\phi \\ 0 & s\phi s\theta & c\phi s\theta \end{bmatrix}\begin{bmatrix}p\\ q\\ r\end{bmatrix}, \qquad (12)$$

where u, v, w are linear velocities in the local body fixed frame along the x, y, z axes, respectively and p, q, r are the angular velocities in the local body fixed frame along the x, y, z axes, respectively. The AUV posture can be defined by six coordinates, 3 representing the position $x_1=(x, y, z)^T$ and 3 corresponding to the orientation $x_2=(\phi, \theta, \psi)^T$, all with respect to the world frame. The variable constraints are provided in Table 1.

Table 3. Simulation parameters

u	[0 2]m/s
v	[-0.1 0.1]m/s
w	[-0.1 0.1]m/s
p	[-5 5]deg/s
q	[-5 5]deg/s
r	[-15 15]deg/s

Fig. 6. A scenario where the AUV has a goal point directly behind the start, but it cannot reverse the vehicle. (3-D Vehicle Path)

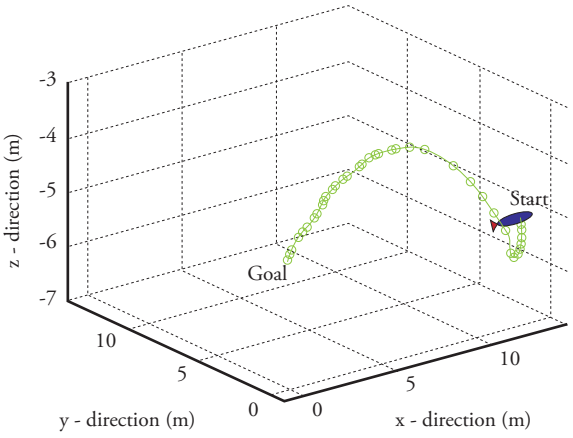

For this simulation the sampling factor was 25. A start posture of (12m, 0m, -5m, 0°, 0°, 0°) was given with a goal point of (0m, 0m, -5m,), which is directly behind the start point. Since the vehicle was constrained to forward velocity along the x-axis it could not reverse to the goal. As Fig. 6 shows, it must turn around to reach the goal. A path planner that considers a vehicle to be holonomic would simply produce a straight line from the start to the goal. However, the ability of SBMPC to consider the vehicle constraints and kinematic model produces a feasible trajectory from the start to the goal.

Conclusions

Sampling-Based Model Predictive Control has been shown to effectively generate a control sequence for an AUV in the presence of a number of nonlinear constraints. SBMPC exploits sampling-based concepts along with the *LPA** incremental optimization algorithm to achieve the goal of being able to quickly determine control updates while avoiding local minima. The SBMPC solution is globally optimal *subject to the chosen sampling method*. When the entire state space is gridded, the SBMPC algorithm guarantees that the algorithm will converge to a solution if one exists.

This paper presents preliminary results using the

2D kinematic model in cluttered environments and a 3D kinematic model in free space. A future goal of this research is to consider 3-D motion utilizing the dynamic model. However, a dynamic model has greater complexity then a kinematic model, which will lead to increased computational times, and difficulties in achieving real time operation. One possible solution is to employ a method that switches from a dynamic model in complex situations to a kinematic model in less complex circumstances.

Currently, the goal region is only concerned with the AUV reaching a certain position. However, in certain missions, such as docking or recovery, it may be necessary for the vehicle to arrive at a specified posture. Consequently, the goal region will include the orientation in future work.

Lastly, because of the constantly changing environment in which the AUV must move, the time varying nature of the AUV dynamics, and the uncertainty of the hydrodynamic coefficients it is important to eventually replan the path. This is one of the benefits of traditional MPC; by replanning at every time step it produces robustness. SBMPC can incorporate replanning through the use of *LPA**.

References

[1] S. TRUVER, *"Mines, improvided explosives: a threat to global commerce?"* National Defense Industrial Association, vol. 91, no. 641, pp. 46–47, April 2007.

[2] A. WILBY, *"Meeting the threat of maritime improvised explosive devices,"* Sea Technology, vol. 50, no. 3, March 2009.

[3] M. CHERIF, *"Kinodynamic motion planning for all-terrain wheeled vehicles,"* Proceeding IEEE International Conference on Robotic and Automation, pp. 317–322, 1999.

[4] H. KAWANO, *"Real-time obstacle avoidance for underactuated autonomous underwater vehicles in unknown vortex sea flow by the mdp approach,"* International Conference on Intelligent Robots and Systems, pp. 3024–3031, October 2006.

[5] O. YAKIMENKO, D. HORNER, and D. P. Jr., *"Auv rendezvous trajectories generation for underwater recovery,"* Mediterranean Conference on Control and Automation, pp. 1192–1197, June 2008.

[6] C. CALDWELL, E. COLLINS, and S. PALANKI, *"Integrated guidance and control of auvs using shrinking horizon model predictive control,"* OCEANS Conference, September 2006.

[7] D. D. DUNLAP, E. G. COLLINS, JR., and C. V. CALDWELL, *"Sampling based model predictive control with application to autonomous vehicle guidance,"* Florida Conference on Recent Advances in Robotics, May 2008.

[8] S. KOENIG, M. LIKHACHEV, and D. FURCY, *"Lifelong planning A*,"* Artificial Intelligence, 2004.

[9] D. DUNLAP, C. CALDWELL, and E. COLLINS, *"Nonlinear model predictive control using sampling and goal-directed optimization,"* IEEE Multiconference on Systems and Control, September 2010.

[10] S. M. LAVALLE, Planning Algorithms. Cambridge University Press, 2006.

[11] J. MACIEJOWSKI, Predictive Control with Constraints. Haslow, UK: Prentice Hall, 2002.

[12] S. M. LAVALLE, *"Rapidly-exploring random trees: A new tool for path planning,"* Iowa State University, Tech. Rep., 1998.

[13] L. E. KAVRAKI, P. SVESTKA, J. C. LATOMBE, and M. H. OVERMARS, *"Probabilistic roadmaps for path planning in high-dimensional configuration spaces,"* IEEE Transactions on Robotics & Automation, vol. 12, no. 4, pp. 566 – 580, June 1996.

[14] M. LIKHACHEV and A. STENTZ, *"R* search,"* Proceedings of the National Conference on Artificial Intelligence (AAAI), pp. 1–7, Apr 2008.

[15] S. R. LINDEMANN and S. M. LAVALLE, *"Incremental low-discrepancy lattice methods for motion planning,"* International Conference on Robotics & Automation, pp. 2920–2927, September 2003.

Editorial Regulations for Authors

Thematic

The *Ship Science and Technology* Journal accepts for publication original engineering contributions in English language on ship design, hydrodynamics, dynamics of ships, structures and materials, vibrations and noise, technology of ship construction, marine engineering, standards and regulations, ocean engineering and port infrastructure, results of scientific and technological researches. Every article shall be subject to consideration of the Editorial Council of *The Ship Science and Technology* Journal deciding on pertinence of its publication.

Typology

The *Ship Science and Technology* Journal accepts publishing articles classified within following typology (Colciencias 2006):

- *Scientific and technological research article*. Document presenting detailed original results of finished research projects. Generally, the structure used contains for important parts: introduction, methodology, results and conclusions.
- *Reflection Article*. Document presenting results of a finished research as of an analytical, interpretative or critical perspective of author, on a specific theme, resorting to original sources.
- *Revision Article*. Document resulting from a finished research in the field of science or technology in which published or unpublished results are analyzed, systemized and integrated in order to present advances and development trends. It is characterized for presenting an attentive bibliographic revision of at least 50 references.

Format

All articles must be sent to editor of *The Ship Science and Technology* Journal accompanied by a letter from authors requesting its publication. Every article must be written in *Microsoft Word* processor in single space and sent in magnetic form. Articles must not exceed 10,000 words (9 pages). File must contain all text and any tabulation and mathematical equations.
All mathematical equations must be written in *Microsoft Word Equation Editor*. This file must contain graphs and figures; additionally, they must be sent in a modifiable format file (soft copy). Also, abbreviations and acronyms have to be defined the first time they appear in the text.

Content

All articles must contain following elements that must appear in the same order as follows:

Title
It must be concise (no more than 25 words) with appropriate words so as to give reader a slight idea of content. It must be sent in English and Spanish language.

Author and Affiliations
Author's name must be written as follows: name, initial of second name and surnames. Affiliations of author must be specified in following way and order:

- Business or institution (including department or division to which he/she belongs).
- Mail address.
- City (Province/State/Department).
- Country.
- Telephone.

Abstract
Short essay of no more than one hundred fifty (150) words specifying content of work, scope and results. It must be written in such a way so as to contain key ideas of document. It must be sent in English and Spanish language.

Key Words
Identify words and/or phrases (at least three) that recovers relevant ideas in an index. They must be sent in English and Spanish language.

Introduction
Text must be explanatory, clear, simple, precise and original in presenting ideas. Likewise, it must be organized in a logic sequence of parts or sections, with clear subtitles that guide reader. The first part of document is the introduction. Its objective is to present the theme, objectives and justification of why it was elected. Likewise, it must contain sources consulted and methodology used as well as a short explanation of status of research if it were the case and form in which the rest of article is structured.

Body Article
It is made up of the theoretical framework supporting the study, statement of theme, status of its analysis, results obtained and conclusions.

Equations, Tables, Charts ang Graphs
All of these elements must be numbered in order of appearance according to its type and have at the foot, that is, exactly underneath of chart, graph or picture, the source from where data was taken and who made it.

Equations must be numbered on the right hand side of column containing it, in the same line and in parenthesis. Body of text must make reference of it as "(Equation x)". When the reference starts a sentence it must be made as follows: "Equation x".

Equations must be written so that capital letters can be clearly differenced from small letters. Avoid confusions between letter "l" and number one or between zero and small letter "o". All subindexes, superindexes, Greek letters and other symbols must be clearly indicated.

All expressions and mathematical analysis must explain all symbols (and unit in which it is measured) that have not been previously defined in the nomenclature. If work is extremely mathematical by nature, it would be advisable to develop equations and formulas in appendixes instead of including them in body of text.

Figure/Fig. (lineal drawings, tables, pictures, figure, etc.) must be numbered according to order of appearance and should include the number of graph in parenthesis and a brief description. As with equations, in body of text, reference as "(Fig. X)", and when reference to a graph is the beginning of a sentence it must be made as follows: "Fig. x".

Charts, graphs and illustrations must be sent in modifiable vector file format (*Microsoft Excel*, *Microsoft Power Period* and/or *Microsoft Visio*). Pictures must be sent in TIF or JPG format files, separate from main document in a resolution higher than 1000 dpi.

Foot Notes
We recommend their use as required to identify additional information. They must be numbered in order of appearance along the text.

Acknowledgment
Acknowledgments may be made to persons or institutions considered to have made an important contribution and not mentioned in any other part of the article.

Bibliographic References

The bibliographic references must be included at the end of the article in alphabetical order and shall be identified across the document. For the citation of references the Journal uses ISO 690 standards, which specifies the mandatory elements

to cite references (monographs, serials, chapters, articles, and patents), and ISO 690-2, related with the citation of electronic documents.

Quotations
They must be made in two ways: at the end of text, in which case last name of author followed by a comma and year of publication followed in the following manner:

"Methods exist today by which carbon fibers and prepregs can be recycled, and the resulting recyclate retains up to 90 percent of the fibers' mechanical properties" *(Davidson, 2006)*.

The other way is:
Davidson (2006) manifests that "Methods exist today by which carbon fibers and prepregs can be recycled, and the resulting recyclate retains up to 90 percent of the fibers' mechanical properties".

List of References
Bibliographic references of original sources for cited material must be cited at the end of article in alphabetical order and according to following parameters:

In the event of more than one author, separate by commas and the last one by an "and". If there are more than three authors write the last name and initials of first author and then the abreviation "et al.".

Books
Last name of author followed by a comma, initial(s) of name followed by a period, the year of publication of book in parenthesis followed by a comma, title of publication in italics and without quotation marks followed by a comma, city where published followed by a comma and name of editorial without abbreviations such as Ltd., Inc. or the word "editorial".

Basic Form:
LAST NAME, N.I. *Title of book*. Subordinate responsibility (optional). Edition. Publication (place, publisher). Year. Extent. Series. Notes. Standard Number.
Example:
GOLDBERG, D.E. *Genetic Algorithms for Search, Optimization, and Machine Learning*. Edition 1. Reading, MA: Addison-Wesley. 412 p. 1989. ISBN 0201157675.

If a corporate author
Write complete name of entity and follow the other standards.

Basic form:
INSTITUTION NAME. *Title of publication*. Subordinate responsibility (optional). Edition. Publication (place, publisher). Year. Extent. Series. Notes. Standard Number.

Example:
AMERICAN SOCIETY FOR METALS. *Metals Handbook: Properties and Selection: Stainless Steels, Tool Materials and Special-Purpose Metals*. 9th edition. Asm Intl. December 1980. ISBN: 0871700093.

When book or any publication have as author an entity pertaining to the state, write name of country first.

Basic form:
COUNTRY, ENTITY PERTAINING TO THE STATE. *Title of publication*. Subordinate responsibility (optional). Edition. Publication (place, publisher). Year. Extent. Series. Notes. Standard Number.

Example:
UNITED STATED OF AMERICAN. EPA - U.S. Environmental Protection Agency. Profile of the Shipbuilding and Repair Industry. Washington D.C. 1997. P. 135.

Journal Article

Basic form:
Last name, N.I. Title of article, *Name of publication*. Edition. Year, issue designation, Pagination of the part.

Example:
SAVANDER, B. R. and TROESCHB. Mission Configurable Modular Craft Concept Study. S*hip Science and Technology*. Year 3, N.° 5, Vol. 1, July 2009, p. 31-56.

Graduation Work

Basic form:
Primary responsibility. *Title of the invention*. Subordinate responsibility. Notes. Document identifier: Country or issuing office. *Kind of patent document*. Number. Date of publication of cited document.

Example:
CARL ZEISS JENA, VEB. *Anordnung zur lichtelektrischen Erfassung der Mitte eines Lichtfeldes. Et-finder*: W. FEIST, C. WAHNERT, E. FEISTAUER. Int. Cl.3 : GO2 B 27/14. Schweiz Patentschrift, 608 626. 1979-01-15.

Presentation at conferences or academic or scientific event

Basic form:
LAST NAME, N.I. Title of the presentation. In: Sponsor of the event. *Name of the event*. Country, City: Publisher, year. Pagination of the part.

Example:
VALENCIA, R., et al. Simulation of the thrust forces of a ROV En: COTECMAR. P*rimer Congreso Internacional de Diseño e Ingeniería Naval CIDIN 09*. Colombia, Cartagena: COTECMAR, 2009.

Internet

Basic form:
LAST NAME, N.I. *Title of work*, [on-line]. Available at: http://www.direccion_completa.com, recovered: day of month of year.

Example:
COLOMBIA. ARMADA NACIONAL. Cotecmar gana premio nacional científico, [web on-line]. Available at: http://www.armada.mil.co/?idcategoria=545965, recovered: 5 January of 2010.

Acceptance

Articles must be sent by e-mail to editor of The *Ship Science and Technology* Journal to otascon@cotecmar.com or in CD to mail address of journal (Cotecmar Mamonal Km 9 Cartagena Colombia), accompanied of the "Declaration of Originality of Work Written "included in this journal. Author shall receive acknowledgement of receipt by e-mail. All articles will be submitted to Peer Review. Comments and evaluations made by the journal shall be kept in confidentiality. Receipt of articles by The Ship Science and Technology Journal does not necessarily constitute acceptance for publishing. If an article is not accepted it shall be returned to the respective author. The Journal only publishes one article by author in the same number of the magazine.

Opinions and declarations stated by authors in articles are of their exclusive responsibility and not of the journal. Acceptance of articles grants The Ship Science and Technology Journal the right to print and reproduce these; nevertheless, any reasonable petition by author to obtain permission to reproduce his/her contributions shall be attended.

Further information can be obtained by:
Sending an e-mail to sst.journal@cotecmar.com
Contacting Oscar Dario Tascón (Editor)
The Ship Science and Technology (Ciencia y Tecnología de Buques) office located at: Cotecmar Mamonal Km. 9 Cartagena Colombia. Phone Number: 57 - 5 - 6685377.

SHIP
SCIENCE & TECHNOLOGY
CIENCIA & TECNOLOGÍA DE BUQUES

Statement of Originality of Written Work

Title of work submitted

_____

_____

_____

I hereby certify that work submitted for publication in The *Ship Science and Technology* journal, of Science and Technology for the Development of Naval, Maritime and Riverine Industry Corporation, Cotecmar, was written by me, given that its content is product of my direct intellectual contribution. All data and references to material already published are duly identified with its respective credit and included in the bibliographic notes and quotations highlighted as such.

I therefore declare that all materials submitted for publication are completely free of copyrights; consequently, I make myself responsible for any lawsuit or claim related with Intellectual Property Rights thereof.

In the event that article is chosen for publication by The *Ship Science and Technology* journal, I hereby state that I totally transfer reproduction rights of same to Science and Technology for the Development of Naval, Maritime and Riverine Industry Corporation, Cotecmar. In retribution for present transfer I agree to receive two issues of the journal where my article is published.

In witness thereof, I sign this statement on the _____ day of the month of _____ of year _____, in the city of _____ .

Name and signature: Identification document:

_____ _____

Km. 9 Vía Mamonal - Cartagena, Colombia
www.cotecmar.com/cytbuques/

Concepts and Conclusions from the "2010 Pan-American Advanced Studies Institute on Dynamics and Control of Manned and Unmanned Marine Vehicles"

Leigh McCue, Marco Sanjuan, Ryan Hubbard

SPH Boundary Deficiency Correction for Improved Boundary Conditions at Deformable Surfaces

Van Jones, Qing Yang, Leigh McCue-Weil

Creating Bathymetric Maps Using AUVs in the Magdalena River

Monique Chyba, John Rader, Michael Andoinian

Metamodeling Techniques for Multidimensional Ship Design Problems

Peter B. Backlund, David Shahan, Carolyn C. Seepersad

Application of Sampling Based Model Predictive Control to an Autonomous Underwater Vehicle

Charmane V. Caldwell, Damion D. Dunlap, Emmanuel G. Collins Jr.

COTECMAR

www.cotecmar.com/cytbuques/